Geological Magazine

www.cambridge.org/geo

The Early Ordovician Middle Shale Member (Am3) of the Amdeh Formation and further evidence of conodont faunas from the Sultanate of Oman

AP Heward[1], CG Miller[2] and GA Booth[3]

[1]23 Croftdown Court, Malvern, WR14 3HZ, UK; [2]Department of Earth Sciences, The Natural History Museum, Cromwell Road, London SW7 5BD, UK and [3]Weyhill, Old Compton Lane, Farnham, Surrey GU9 8EG, UK

Original Article

Cite this article: Heward AP, Miller CG, and Booth GA. (2019) The Early Ordovician Middle Shale Member (Am3) of the Amdeh Formation and further evidence of conodont faunas from the Sultanate of Oman. *Geological Magazine* **156**: 1357–1374. doi:10.1017/S0016756818000729

Received: 14 June 2018
Revised: 21 September 2018
Accepted: 24 September 2018
First published online: 26 November 2018

Keywords:
trace fossils; conodonts; spectral gamma ray; heavy minerals; Tremadocian; Floian

Author for correspondence:
AP Heward, Email: alan@midfarm.demon.co.uk

Abstract

The Middle Shale Member of the Amdeh Formation is interpreted to be of Early Ordovician age based on its trace fossils, stratigraphic context and a newly discovered fauna of conodonts. The member abruptly overlies the Lower Quartzite Member, which may be Early Cambrian, and passes gradationally-upward into the Upper Quartzite Member, which is probably Early–Middle Ordovician. The 542.5 m thick Middle Shale Member can be divided into two parts: a shaly lower part, and a sandy upper part that contains an influx of heavy minerals. Bioturbation by marine trace fossils is one of the most obvious characteristics of the member. The shales and sandstones are interpreted to be of *Cruziana* and *Skolithos* ichnofacies and represent shallow-marine shelf, shoreface, beach and coastal deposits. Sparse shelly fossils occur in the sandy upper part, principally bivalves, inarticulate brachiopods, ostracods and conodonts. The small assemblage of conodonts includes elements interpreted to be Tremadocian (*Tetraprioniodus*, *Drepanoistodus*, *Drepanodus*, *Scolopodus*, ?*Tropodus*, *Semiacontiodus* and *Teridontus*), and others which may be Floian or ancestral forms of Floian taxa (Balognathidae gen. et sp. indet. A & B and aff. *Erraticodon*). No acritarchs have been recovered, probably due to high temperatures experienced during burial to >6 km. It is likely that the Middle Shale Member is the seaward equivalent of the Mabrouk and Barakat formations, and an outcrop gamma-ray log supports such a correlation. The trace fossils, sedimentology, conodont fauna and the general lack of macrofossils are in keeping with the regional Tremadocian–Floian of the Arabian margin of Gondwana.

1. Introduction

Deposits of Ordovician age in the Sultanate of Oman have been recognized from oil and gas exploration activities over the past 60 years (Morton, 1959; Hughes Clarke, 1988; Droste, 1997; Molyneux *et al.* 2006; Forbes *et al.* 2010). Cores from this interval have yielded graptolites, *Cruziana*, conodonts and fragments of some of the earliest land plants (Morton, 1959; HA Armstrong, unpub. report, 1993; C Burrett, unpub. note, 1993; Wellman *et al.* 2003; Rickards *et al.* 2010). The deposits occur mainly in the subsurface of the north and west of Oman, south of the Hawasina front of the Al Hajar mountains (Fig. 1a). They also crop out in the Saih Hatat window of the eastern Al Hajar, in the Qarn Mahatta Humaid area on the flank of the Ghaba Salt Basin, and in the Dibba Zone in the United Arab Emirates (UAE) (Figs 1a and 2). The history of research on the outcrops in Saih Hatat has been summarized by Heward *et al.* (2018). A type section of 3.4 km thickness of Amdeh Formation was measured in Wadi Qahza (Khaza) by Lovelock *et al.* (1981). Five members were distinguished, three shaly and two intervening ones of quartzite which form ridges, gorges and hills. An Early Ordovician age was interpreted for the formation, based on rare acritarchs, trilobites and trace fossils. Geologists from the Bureau de Recherches Géologiques et Minières (BRGM) remapped the area and, for simplicity, abbreviated the names of the five members to Am1–Am5 (Le Métour *et al.* 1986; Villey *et al.* 1986). The Amdeh Formation, on the southern side of the Saih Hatat window, has been subjected to greenschist-facies metamorphism (Breton *et al.* 2004; Searle *et al.* 2004). The effects of this are the development of a single slaty cleavage in the shales and a fracture cleavage in the sandstones (Le Métour *et al.* 1986). Zircon and apatite fission-track studies on samples from the Amdeh Formation close to Wadi Qahza indicate peak temperatures of 200–300 °C during deep burial in the Late Cretaceous, followed by two periods of cooling due to uplift in the Cretaceous and mid-Cenozoic (Saddiqi *et al.* 2006; Hansman *et al.* 2017).

Little detailed stratigraphical or sedimentological work has been carried out on the bulk of the outcropping Amdeh Formation, possibly because of its daunting thickness, its metamorphic overprint that increases to the NE, and its lack of age-diagnostic macro-fossils. Marine trace fossils abound in the upper three members of the formation (Am3–5; *Skolithos*, *Daedalus*,

CAMBRIDGE UNIVERSITY PRESS

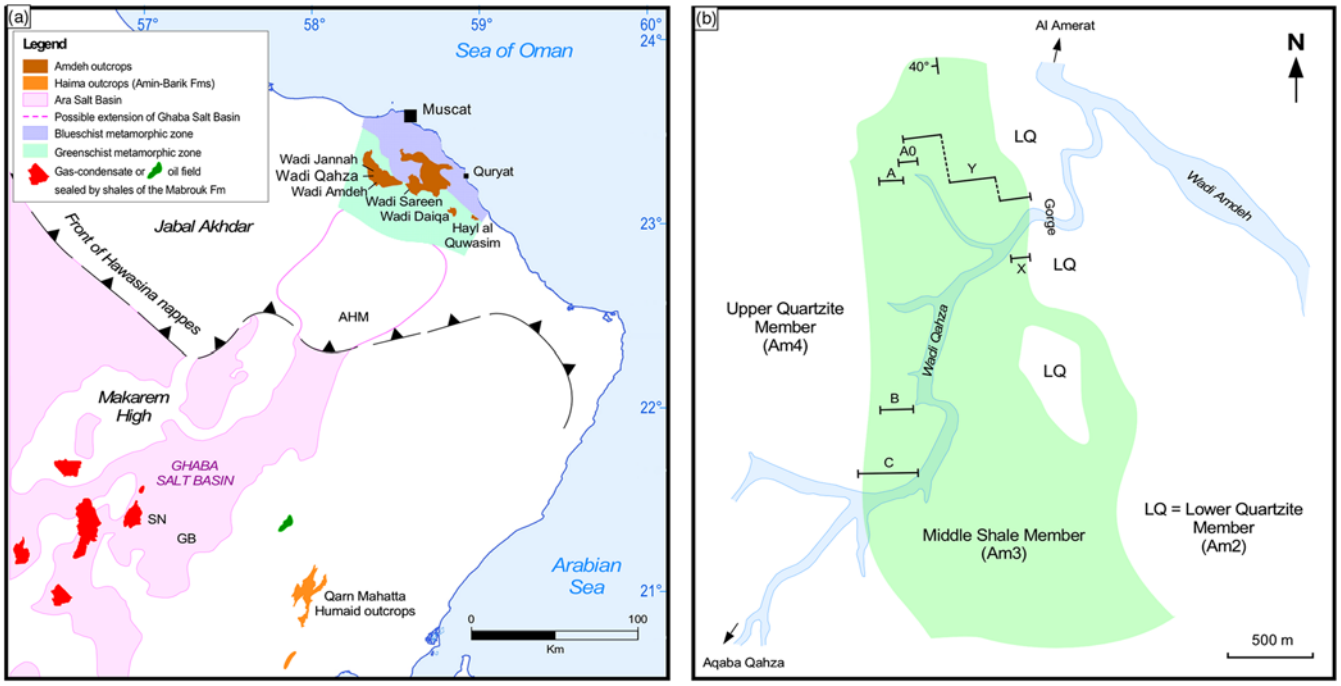

Fig. 1. (a) Outcrops of the Amdeh Formation on the southern rim of the Saih Hatat window of the Al Hajar Mountains, Oman. Outcrop outlines and metamorphic zones are from BRGM mapping. The gas-condensate and oil fields marked are those sealed by shales of the Mabrouk Formation. GB, SN and AHM are well locations referred to in the text and on figures. (b) Location of measured sections in Wadi Qahza. The coordinates of sample locations and the bases and tops of sections are listed in the Appendix.

Cruziana, *Phycodes*, *Teichichnus*), and two species of *Daedalus* (*D. labechi*, *D. desglandi*) were described based on examples from Wadi Qahza (Seilacher, 2000).

Acritarchs and chitinozoans are the prime tools of biostratigraphy in the subsurface Ordovician of Oman, and the failure to recover them in many samples from the outcropping Amdeh Formation has frustrated and hindered understanding. The exceptions are from Am5 deposits in the easternmost inliers of Wadi Daiqa and Hayl al Quwasim where several good assemblages have now been obtained (Fig. 1a; Heward *et al.* 2018). A Darriwilian age for this shaly Am5 Member has been firmly established based on these floras, equivalent to the Saih Nihayda Formation in the subsurface of northern Oman (Fig. 2).

This paper describes the next oldest shaly interval, the Middle Shale Member or Am3. The paper provides evidence of its Early Ordovician age (Tremadocian–Floian) and its equivalence to the subsurface Mabrouk and Barakat formations of the Ghaba Salt Basin (Fig. 2). The Mabrouk Formation is the top seal for gas-condensate and oil trapped in Barik Sandstone reservoirs in the basin (Fig. 1a). The recovery of a conodont fauna from outcrop samples, together with an unpublished one from a 1958 core from the subsurface, indicates promise for further interesting discoveries at a time of major divergence and diversification of conodont faunas (Dzik, 2015).

2. Materials and methods

Six sections were measured in Wadi Qahza, two in the shalier lower part of the Middle Shale Member (X and Y) and four in its sandier upper part (A0, A, B and C; Fig. 1b). Ichnofabric index was estimated using the scheme of Bottjer & Droser (1991, fig. 1). The sections were also logged with a RS-230 portable spectral gamma-ray (GR) tool at 0.5 m intervals. Logging the sections with a portable GR was originally intended to aid correlation with the subsurface of the Ghaba Salt Basin in the presumed absence of age-diagnostic fossils, but revealed a significant change in sediment provenance that would otherwise have gone unrecognized. A 30 s period was used for assaying potassium, uranium and thorium (K, U, Th). A standard conversion of 8*U ppm + 4*Th ppm + 16*K % was used to compute GR values in API (American Petroleum Institute) units (wikipedia.org/wiki/Gamma_ray_logging). It was found, though, that an adjustment of 4* rather than 16*K produced API values more comparable with those of probable equivalents in the subsurface at depths of 4–5 km. This seemed reasonable given an increase in illite with burial depth in the presence of continuing input of potassium from degrading feldspar (Aplin & Macquaker, 2011). Standard API conversion values and ones adjusted for potassium are quoted in the subsequent text and displayed in Figures 4 and 8.

The measured sections were linked by walking out marker beds and converted to true thickness using UTM coordinates from GPS and average dips. Thicknesses are considered accurate to ±20%. Marker beds and units were also located and traced in sections in Wadi Jannah 4 km to the NW and Wadi Amdeh 6 km to the SE (Fig. 1a).

Thirteen thin-sections were prepared to aid the study, and carbonate ones were stained with Alizarin red S and potassium ferricyanide to distinguish carbonate minerals. Five samples of calcareous lithologies were processed for conodonts and, despite a previous lack of success, three samples of promisingly dark shales for palynology (see Appendix for locations). The conodont samples were dissolved using 10% acetic acid and the 75 μm to 2 mm residue separated using a solution of sodium polytungstate at a specific gravity of 2.80 g cm^{-3}. When a few

https://doi.org/10.1017/S0016756818000729 Published online by Cambridge University Press

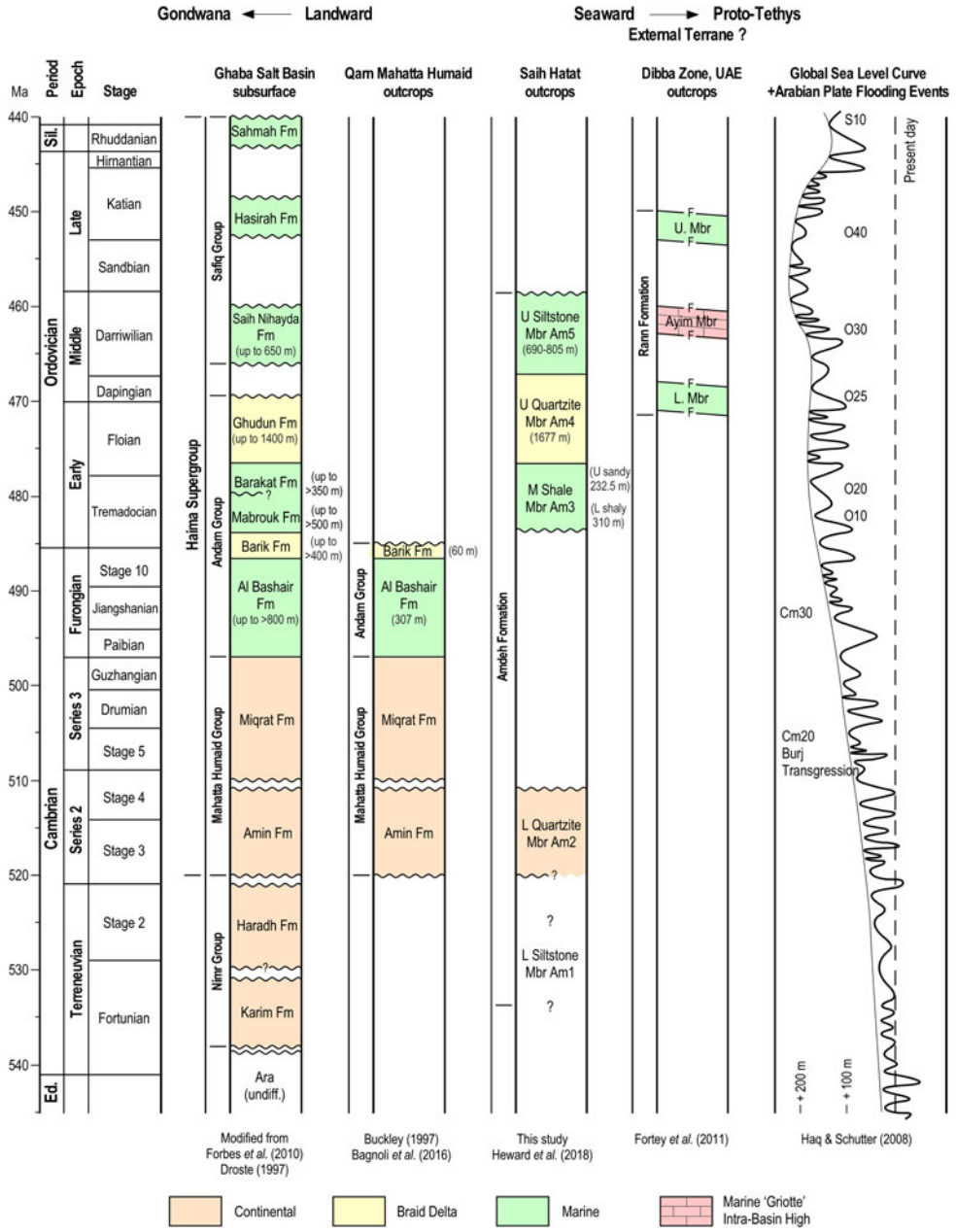

Fig. 2. Summary stratigraphy of the Cambrian and Ordovician of Oman and the neighbouring Dibba Zone of the UAE; Buckley (unpub. Ph.D. thesis, Birbeck Coll., Univ. of London, 1997). The surface outcrops and subsurface equivalents in the Ghaba Salt Basin are shown in relation to the global sea-level curve and the main flooding events identified from the Arabian Plate. With the overall rise of global sea-level, continental deposits are progressively replaced by marine ones. More diverse Tremadocian–Floian faunas are reported from Iran and Turkey, from the external terranes of Gondwana, and may indicate that the fossiliferous Rann Formation outcrops in the UAE also represent deposits of an external terrane.

conodont elements were found in the residue of a partially dissolved 477 g sample of shelly sandstone, the remaining pieces of sample were exposed to more than 20 freeze–thaw cycles, resulting in 355 g of sample being broken down. The entire 75 µm to 2 mm residue was then picked unseparated and yielded 26 fragmentary specimens (est. 73 specimens per kg). The Conodont Alteration Index (CAI) was calculated using the method of Epstein *et al.* (1977).

The outcrops of the Amdeh Formation in Wadi Qahza are cut by dolerite dikes, as elsewhere in the SW of Saih Hatat. The dikes are green, highly altered, 5–10 m wide, trend NW to SE and are spaced at hundreds of metres (Fig. 3a). They are probably of Permian age and related to two intervals of rift-related volcanism that occur in the same area interbedded with carbonates of the overlying Saiq Formation (Chauvet *et al.* 2009).

3. Sedimentology and log character

3.a. Description

The Middle Shale interval forms low ground between an imposing ridge of the Lower Quartzite and the first cliff-forming sandstones of the Upper Quartzite (Fig. 3a, c). At 542.5 m, it is thicker than the 445 m recorded by Lovelock *et al.* (1981), mainly because the top of the member has been revised upward to a widespread marine marker that is also more in keeping with the definition of subsurface formations. The Middle Shale can be divided into a shalier lower part (1) and a sandier upper part (2) and, within those, seven units are distinguished based on sand content, colour and GR response (1.1–1.3 and 2.1–2.4; Fig. 4). The average concentrations of K are 3.9%, U 4.2 ppm and Th 16.4 ppm and there is a noticeable increase in thorium

https://doi.org/10.1017/S0016756818000729 Published online by Cambridge University Press

Fig. 3. The Middle Shale Member (Am3) in Wadi Qahza. (a) Overview of the lowermost shalier units in Wadi Qahza showing subdued topography, lateral continuity of beds and intervals of different colour, green-brown, grey-purple and green-brown. The underlying Lower Quartzite Member (LQ) forms a prominent ridge and wadi gorge to the right. (b) Overview of upper sandier part with two sandstone-dominated intervals (2.2 and 2.4) separated by a finer-grained one (2.3). (c) The uppermost part of the Middle Shale and the gradual transition to the first cliff-forming sandstones of the Upper Quartzite Member (UQ). The base of the latter is redefined from the *Cruziana* Marker of Lovelock *et al.* (1981) to the more widespread Shelly Marker.

between the lower (14 ppm) and upper parts (21 ppm) of the succession (Fig. 4).

Much of the Middle Shale interval is thoroughly bioturbated, with the ichnofabric index ranging from 5 to 3 in the lower shaly part and 1 to 5 in the upper sandy part. There is a succession of marine trace fossils, initially *Skolithos* and *Cruziana*, and subsequently *Phycodes*, *Daedalus* and *Teichichnus* (Fig. 4). *Cruziana* are common in shalier intervals, or in sandier beds just below them. *Cruziana furcifera* is the most common form (54%), with *C. rugosa* (18%) and *C. goldfussi* (16%) less common, though in any given interval either of these three species may predominate.

1.1 (54.5 m)

The base of this unit is a major lithological change from the pale-coloured, tightly cemented, sandstones of the Lower Quartzite, to the green, bioturbated, shaly sandstones of the Middle Shale (Fig. 3a). The contact is not obviously erosive or unconformable with any angular discordance. Scattered granules, pebbles and cobbles of chert, quartz and sandstone occur at the contact and for several metres into the overlying beds. Pebble-sized moulds imply that softer clasts, possibly carbonates or shales, were also present and have weathered away. The main part of the unit consists of dm–m beds of bioturbated sandstone with thinner green siltstone beds. The

https://doi.org/10.1017/S0016756818000729 Published online by Cambridge University Press

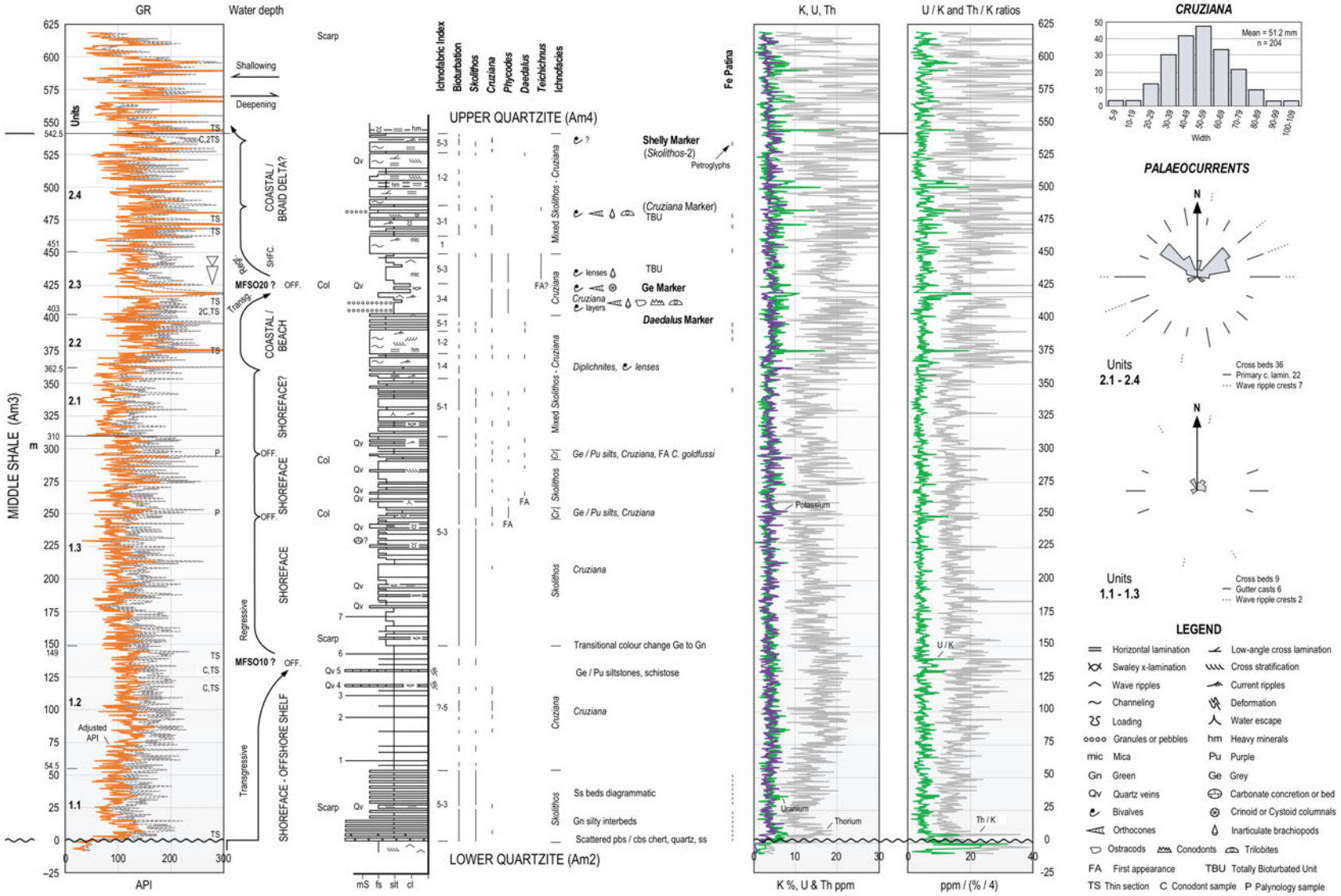

Fig. 4. Composite measured section and gamma-ray (GR) profile through the Middle Shale Member (Am3) in Wadi Qahza. Carbonate beds in units 1.2 and 1.3 are numbered 1–7. The Middle Shale Member has a much higher GR than the thick quartzose sandstones of the Lower and Upper Quartzite Members. There is a noticeable 40–50 API shift in GR over units 2.2–2.4, reflecting an overall increase in thorium and uranium due to an influx of heavy minerals.

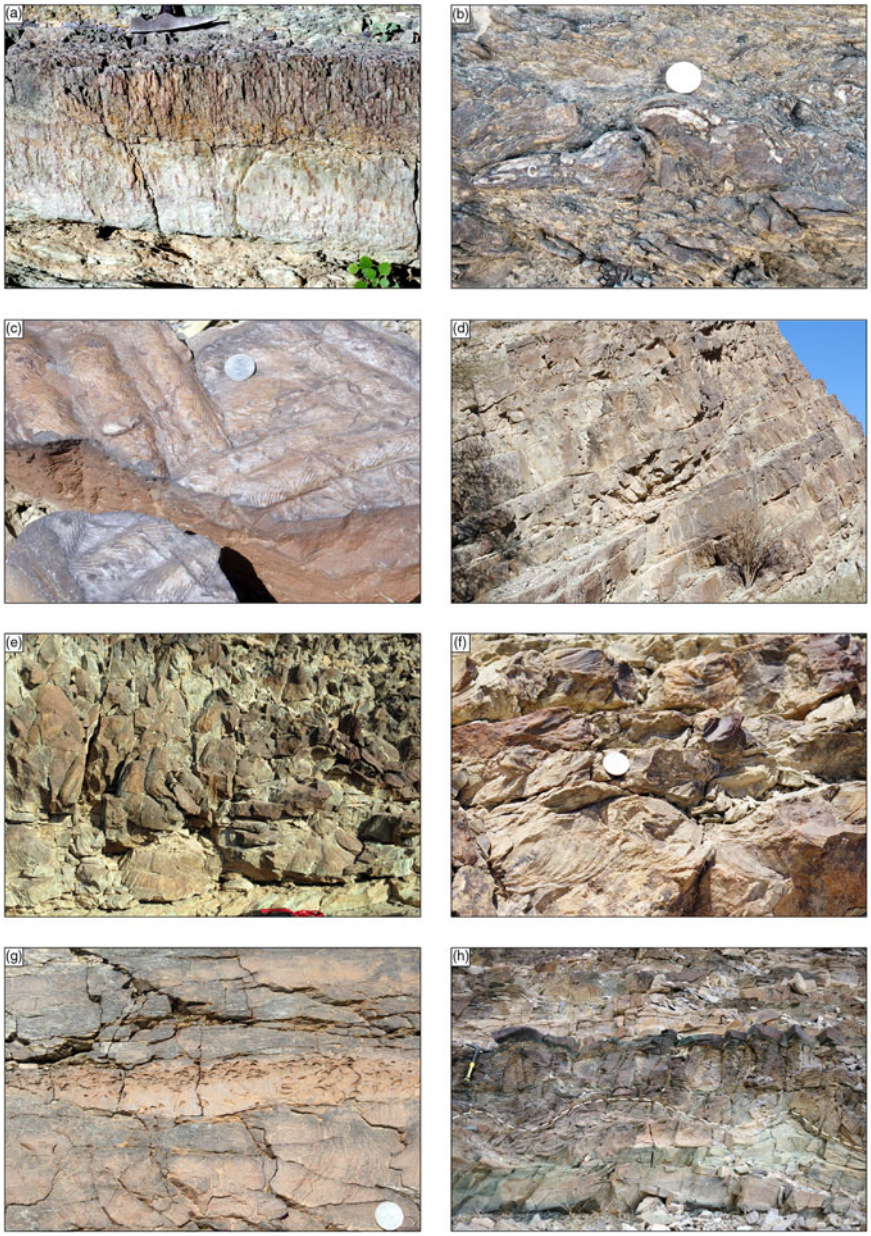

Fig. 5. Outcrop photographs of typical features of the Middle Shale Member, in stratigraphical order. Wadi Qahza except where indicated. Scales: hammer handle 280 mm long, head 175 mm, compass top 75 mm and coin 24 mm across. (a) *Skolithos* burrows cutting through sandstone bed in unit 1.1 (b) Deformed carbonate and quartz-veined horizon 4 within unit 1.2. c = recrystallized carbonate, q = quartz. (c) *Cruziana goldfussi* on the base of sandstone bed from the upper thin grey-purple interval in unit 1.3. (d) Shallow channels in unit 2.2, Wadi Jannah. Metre-thick sandstone beds. (e) *Daedalus* Marker Bed, unit 2.2, containing both *D. labechi* and *D. desglandi*. Note stacked conical texture and the iron patina that is typical of such beds. (f) *Phycodes*, common in dm-thick sandstones beds in units 1.3–2.3. Often also seen as curved mm-wide traces on bedding surfaces. (g) Carbonate concretion within siltstones of the TBU of unit 2.3. The concretion has formed around a lens of bivalve shells, now moulds, that are convex-up and current-packed towards the top. (h) Dewatering structures in a flat-based, flat-topped sandstone immediately overlying the Shelly Marker. Dewatering structures are common in unit 2.4 and throughout the overlying Upper Quartzite. The dark-coloured capping bed, on which the hammer rests, is a heavy mineral placer (Fig. 6f, GR spike rich in U and Th at 544 m on Fig. 4).

sandstone beds are laterally extensive over hundreds of metres and are often coated in an iron patina (Fig. 3a). Rare lighter-colour beds preserve primary sedimentary structures (parallel lamination and current-formed cross-bedding). They are also quartz-veined along a widely spaced fracture cleavage. *Skolithos* burrows are the dominant trace (Fig. 5a), but there is no evidence of these burrows penetrating down into the uppermost sandstones of the underlying Lower Quartzite. Fragmentary *Cruziana* (*C. furcifera and C. rugosa*) are found through the unit, with the lowermost occurrence in a thicker shale bed at 7 m (Fig. 1b, section X). Notably, there is no evidence of the distinctive curving tracks of *Cruziana semiplicata* or the rarer, three-grooved, claw marks of *C. omanica* (Seilacher, 1962, 1970, 1991, 2007). Both the latter species are typical Upper Cambrian forms (Seilacher, 2007, pp. 192–3).

The GR log response shows a marked positive shift of >60 API from the uniform low readings of the underlying Lower Quartzite Member (Fig. 4). The GR ranges from 100 to 175 API units (average 140 API, adjusted 95 API), highest in basal granular sands and lowest in clean quartzose sandstones. A slight enrichment in uranium is present in the coarser-grained basal beds.

1.2 (94.5 m)

This unit consists of grey-purple cleaved shales and siltstones, and thin sandstones (Figs 3a and 4). The shales have a steeply dipping slaty cleavage, and some finer-grained intervals appear schistose. Rarer sandstone beds are bioturbated, with *Cruziana* being the dominant trace (*C. furcifera*, *C. rugosa*, *C. imbricata?*). Bed-parallel quartz veins occur, some associated with thin, 10–100 mm beds of carbonate (Fig. 5b). The carbonates are tabular in form, rather than nodular or concretionary, can be walked out over hundreds of metres laterally and appear to occur at similar levels in sections separated by kilometres. They are laminated and granular, rather than fibrous calcite beef, and lack obvious bioclasts. At least two

https://doi.org/10.1017/S0016756818000729 Published online by Cambridge University Press

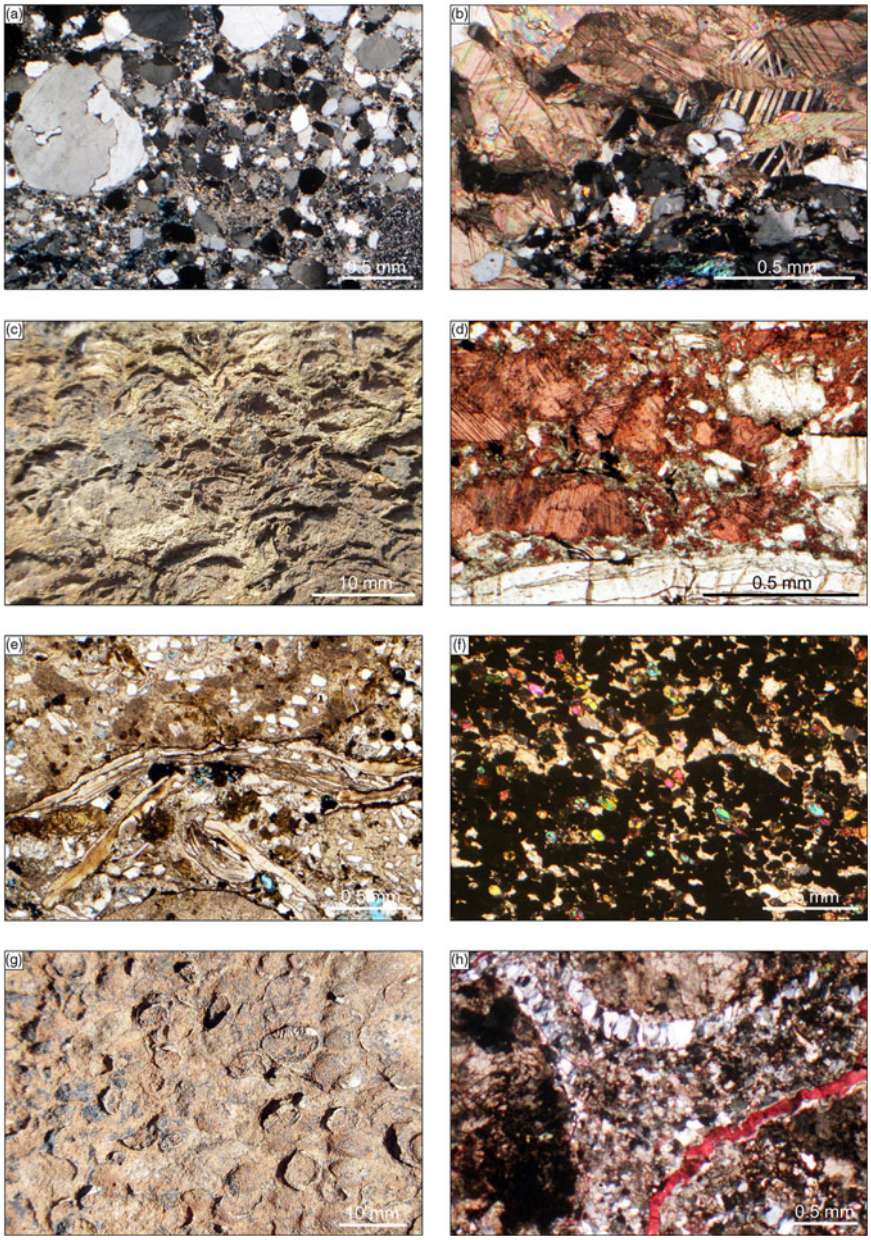

Fig. 6. Thin-section and hand specimen views of distinctive lithologies of the Middle Shale succession. (a) Cross-polarized light (xpl) view of poorly sorted sublitharenite from just above the base of unit 1.1 in section X. Subangular-rounded framework grains of quartz, polyquartz and chert in an illitic matrix. (b) Carbonate horizon 4 in unit 1.2, section Y (Fig. 1b). Large crystals of calcite cement of a fine-grained sandstone (xpl). The appearance of the calcite twins is in keeping with burial temperatures exceeding 200 °C (Burkhard, 1993). (c) Hand specimen of thin, tabular, shell bed in unit 2.3, section A. Convex-upward packing of bivalve shells, seen as moulds on the weathered surface. (d) Thin-section of same in plane-polarized light (ppl), showing bivalves preserved as coarsely-crystalline calcite (red stain), but also abundant, pale-coloured, shell fragments (including inarticulate brachiopods and possible conodonts). (e) Granule-size intraclasts and phosphatic shell debris in a siltstone of unit 2.3, section B (ppl). Variety of intraclasts: massive, granular, porous, pelloidal and ones containing 100 μm-size spherules of radiating clay minerals. (f) Parallel-laminated heavy mineral placer (Fig. 5h), in xpl, just above unit 2.4 in section C, but typical of thinner examples within the unit. Opaque minerals are abundant, as are anatase (rutile?) and zircon. Matrix is of clay minerals. (g) Small silicified bivalve shells, which occur in lenses in the Shelly Marker at the top of unit 2.4, section C. Several shells show dentition-like features. (h) Thin-section of same in xpl revealing that the carbonate is mainly dolomite, cut by thin veins of calcite (red stain) and that the bivalve shells are replaced by a drusy quartz cement.

of them are disharmonically folded on a small scale and have pods of grey recrystallized carbonate and veins of white quartz. In thin-section they consist of coarsely crystalline calcite cement with scattered siltstone grains (Fig. 6b). Samples from two of the carbonate beds (4 and 5) were processed for conodonts but yielded no phosphatic residue.

There is a 20 API positive shift of GR over this interval (avg. 160 API, adj. 115 API) due to its increased shaliness. The colour change from green to grey-purple shales occurs about 20 m before a minor increase in potassium (+0.4%) and thorium (+4.4 ppm).

1.3 (161 m)

The base of unit 1.3 is a small scarp formed by a stack of m-thick sandstones. There is an accompanying colour change back to green, which appears first in the sandstones and then later in the interbedded shales. Some of the thicker sandstone beds (1–5 m) appear to coarsen upward. *Skolithos* is again the dominant trace and some occurrences are gracefully slender, yet more than 650 mm long. A few thicker sandstone beds lack bioturbation and preserve primary sedimentary structures (horizontal, swaley or trough cross-stratification, gutter casts, loading and dewatering features). Such quartzose sandstones are again lighter-coloured, cut by quartz veins along fracture cleavage and often form landscape features or small cliffs. There are two 7–10 m thick reversions to grey-purple shales with abundant *Cruziana*. The first is traceable over kilometres between sections, and marks the appearance of Arthrophycid burrows (*Phycodes*, and then *Daedalus* 17 m upsection in the overlying sandstones). The second grey-purple shale is less laterally continuous and marks the appearance of abundant *Cruziana goldfussi* (Fig. 5c). Three samples of dark-grey siltstone from these intervals were processed for palynology. They yielded only small amounts of totally carbonized organic matter, with no hint of the form of acritarchs.

https://doi.org/10.1017/S0016756818000729 Published online by Cambridge University Press

This unit shows a small negative shift in GR to a range of 100–200 API units (avg. 150 API, adj. 100 API). The grey-purple shaly intervals are noticeably richer in potassium (Fig. 4; K > 7.5%).

2.1 (52.5 m)

Unit 2.1 marks a transition from a shaly bioturbated sequence below to a sandy one above with more preserved primary stratification (parallel lamination, ripple and swaley cross-lamination). *Skolithos* and *Cruziana* continue to dominate, but for the first time distinctive, homogenized beds of *Daedalus* also occur. A sandstone above a green shale at the top of the unit is criss-crossed at its base by narrow tracks of *Diplichnites* (often a single lobe of the trace-maker grazing the surface; Seilacher, 2007, pp. 25–7). Moulds of bivalve shells occur at a similar level in section C (Fig. 1b) and mark the first appearance of body fossils in the Middle Shale Member.

This is the interval with the lowest GR in the Middle Shale Member, with a further small negative shift in the GR (Fig. 4; avg. 140 API, adj. 90 API). Thorium levels are on average 2 ppm less than those of the underlying unit and, surprisingly, 8 ppm less than those of the overlying unit.

2.2 (40.5 m)

Unit 2.2 consists of fine- to medium-grained sandstones with thin interbeds of green-grey shale (Figs 3b and 5d). There are thick intervals with primary stratification, and bioturbation tends to be concentrated in thoroughly churned beds. Parallel lamination, trough cross-stratification (to NW), low-angle cross-stratification (to NE), ripple cross-lamination and metre-scale channelling are the main sedimentary features (Fig. 5d). Laminae of dark-coloured heavy minerals are evident for the first time. *Daedalus* is the most prominent trace fossil and there are several distinctive *Daedalus* beds, one of which forms a marker, which can be traced over kilometres between sections (Fig. 5e) This bed is so homogenized and consolidated that it frequently forms the caprock of dry waterfalls in wadis and of low hills. *Cruziana* occur in most of the shaly interbeds (*C. furcifera* and *C. rugosa*).

Despite being sandy and coarser-grained, this unit, surprisingly, has one of the highest GRs of the Middle Shale Member due to an influx of thorium- and uranium-bearing minerals (Fig. 4; GR range 150–250 API, avg. 185 API, adj. 135 API). One, metre-thick, rippled sandstone peaks at 544 API (3.5% K, 89 ppm Th and 17 ppm U). In thin-section this fine-grained sandstone is rich in heavy minerals.

2.3 (48 m)

This is a distinctive, fine-grained, tripartite interval whose extent can be followed from mountain tops and often from satellite images (Fig. 3b). The lower part of the interval comprises shales, dm-thick sandstones and mm-thick, flaggy, current-packed, beds or lenses of *Redonia*-like bivalves. Bioturbation abounds, *Phycodes* at some levels and *Cruziana* at others (*C. furcifera*, *C. rugosa*). In Wadi Jannah, fallen blocks of a sandstone bed reveal a 'swarm' of aligned *Cruziana* with tracks in either direction. The bivalve beds appear monotaxic in the field, but in thin-section also contain fragments of smaller non-calcitic shells (Fig. 6c) including possible coniform conodonts. Subsequent re-picking of a residue of one of these thin shelly sandstones, sampled due to its obvious Lingulid debris, resulted in the discovery of conodont elements within a fauna of inarticulate brachiopods, ostracods, articulate brachiopods and rare fragments of trilobite (Fig. 7; Appendix). Stringers of granule-sized intraclasts occur at several levels within the shales (Fig. 6d) and in thin-section also contain phosphatic shell debris. Some sand beds have wave-rippled tops (crests orientated ENE–WSW) and others have scattered shell moulds (bivalves, orthoconic nautiloids, and columnals and pluricolumnals of crinoids or cystoids).

The middle part of unit 2.3, the Grey (Ge) Marker, is a light, colour-bleached shale that forms a low, poorly exposed, feature across the outcrops, often followed by modern animal tracks (Fig. 3b). This shale is a décollement interval with discoloration due to fluid movement and quartz veining.

The upper part of unit 2.3 is a Totally Bioturbated Unit (TBU). It is darker-coloured and comprises several metre-thick coarsening-upward cycles separated by thin, laterally continuous, shales (Fig. 3b). *Teichichnus* is the dominant burrow in addition to *Cruziana* and *Phycodes*. Lenses of current packed bivalves continue to occur (Fig. 5g). The shales of unit 2.3 have been searched for graptolites, thus far without success.

This fine-grained interval has a slightly higher GR than the underlying one (Fig. 4, range 150–250 API, avg. 190 API, adj. 140). There are peaks of potassium (7%) in the Grey Marker, and thorium (50 ppm) and uranium (11 ppm) in sandy shales beneath that are deeply churned by *Cruziana*.

2.4 (91.5 m)

Unit 2.4 is predominantly sandy, with thick intervals lacking bioturbation. Cross-bedding, current ripples and horizontal lamination are the main forms of stratification, along with syn-sedimentary loading and dewatering (Fig. 5h). Beds with dewatering features are local in occurrence and are not correlatable laterally between wadi sections hundreds of metres apart. Dark, heavy mineral-laminated sandstones and dm-thick, lens-shaped placers occur. Several dark-grey siltstone intervals are present, one of which is a thinner repeat of the TBU with a granule layer near its base that contains fossil moulds and phosphatic shell debris. *Cruziana* are locally abundant in shaly interbeds and are notable for the range of sizes that co-occur (*C. furcifera*, *C. goldfussi*, *C. rugosa*, 0.5–8 cm wide; cf. discussion in Heward *et al.* 2018). *Skolithos* is present in two beds, and *Daedalus* makes a local reappearance in one of them. The uppermost *Skolithos* bed (*Skolithos*-2 of Lovelock *et al.* 1981) is sufficiently homogenized and smooth that its iron-rich patina has been pecked for rock art at the side of the wadi.

A 5 m thick green shaly interval at the top of the unit contains several horizons of small (<5 mm) bivalves. These occur as moulds in sandstone or as silicified infills in lenses of rotten, brown, dolomitic limestone (Fig. 6g, h). A sample of carbonate was processed for conodonts, but yielded no phosphatic residue. This Shelly Marker, lying above a well-developed *Skolithos* bed, can be traced for >6 km between sections and neighbouring wadis. The *Cruziana* Marker, chosen by Lovelock *et al.* (1981) as the top of the Middle Shale Member, is of local occurrence in section C only and cannot be followed laterally for more than a few tens of metres with any confidence (Fig. 3c).

The GR response over this interval varies from 120 to 250 API (avg. 185 API, adj. 140). Some of the thicker sandstone units are of lower GR (adj. 50–70 API; e.g. that at 524 m, Fig. 4). Occasional GR spikes coincide with heavy mineral placers or with beds with a strong iron patina. A thin-section of the heavy mineral placer shown in Figure 5h (613 API, 5.2% K, 95 ppm Th, 19 ppm U) contains >50% heavy minerals of which >50% are opaque (Fig. 6f). Analysis of two placers in the basal part of the Upper Quartzite

https://doi.org/10.1017/S0016756818000729 Published online by Cambridge University Press

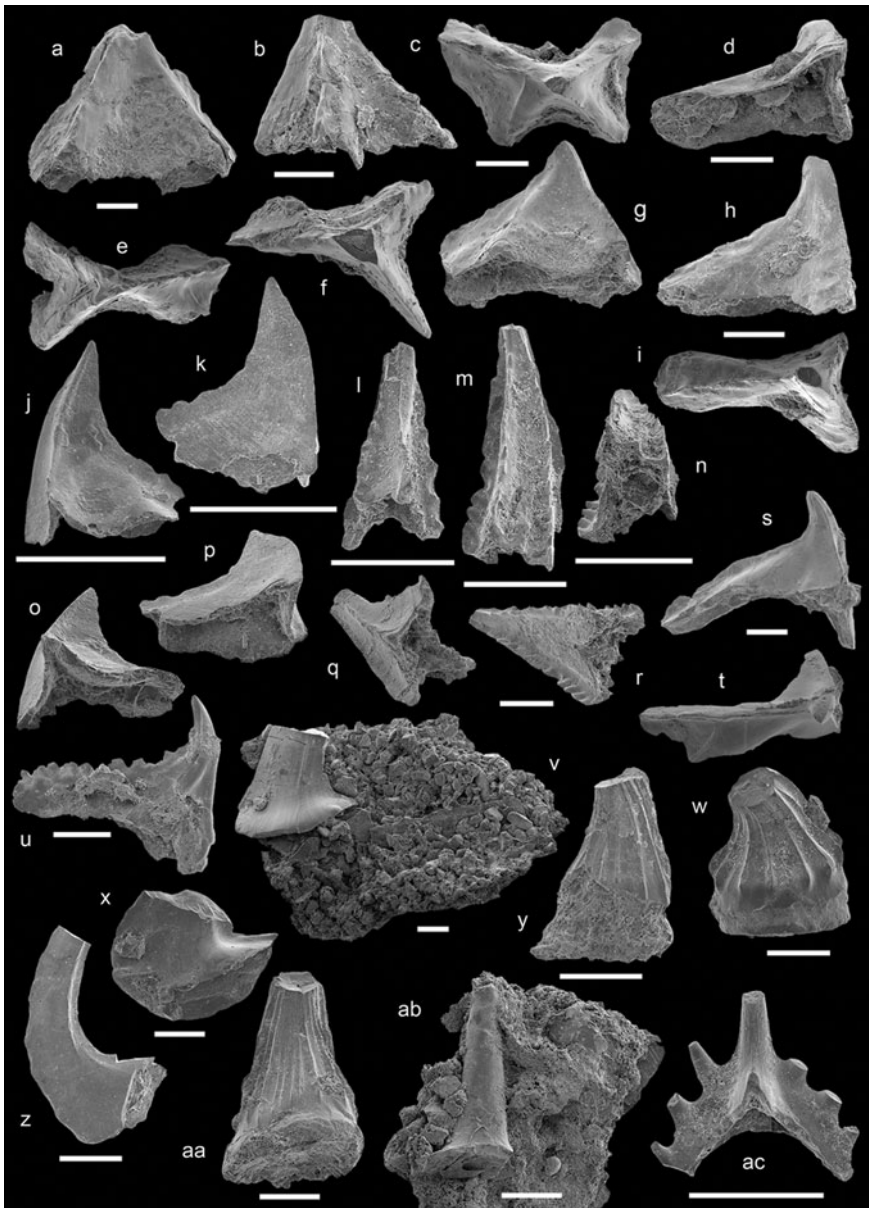

Fig. 7. SEM images of conodonts from sample 16/5, Section B (see Appendix for location). All scale bars are 200 µm. (a–i, s, t) Balognathid gen. et sp. indet. A: P element, (a, e) NHMUK PM X 3965, (a) lateral view, (e) oral view. (b, f) P element, NHMUK PM X 3966, (b) lateral view, (f) oral view. (c, g) P element, NHMUK PM X 3967, (c) lateral view, (g) oral view. (d, h, i) P element, NHMUK PM X 3968, (d) aboral view, (h) lateral view, (i) oral view. (j, k, o, p) Balognathid gen. et sp. indet. B: P element, NHMUK PM X 3969, (j, k) lateral views, (o, p) oblique aboral views. (l, q) Sd element, NHMUK PM X 3970, (l) lateral view, (q) oblique aboral view. (m, n, r) Sd element, NHMUK PM X 3971, (m) lateral view, (n, r) oblique aboral view. (s, t) Balognathid gen. et sp. indet. A, P element, NHMUK PM X 3972, (s) lateral view, (t) oral view. (u) *Tetraprioniodus* sp. P element, NHMUK PM X 3973, lateral view. (v) *Drepanoistodus* sp. suberectiform (p) element embedded in sediment, NHMUK PM X 3974. (w) *Scolopodus* sp. compressed paltodiform element NHMUK PM X 3975. (x) *Drepanodus* oistodiform (r) element, NHMUK PM X 3976. (y) *Semiacontiodus* paltodiform element, NHMUK PM X 3977. (z) *Drepanodus* acontiodiform element NHMUK PM X 3978. (aa) *Semiacontiodus* paltodiform element NHMUK PM X 3979. (ab) *Teridontus* sp. P element, NHMUK PM X 3980. (ac) aff. *Erraticodon* S_0 element, NHMUK PM X 3981, lateral view.

Member (Am4) shows anatase, ilmenite, zircon, haematite and chlorite in a matrix of muscovite and anatase (Mattern *et al.* 2018).

3.b. Interpretation

The abundance of trace fossils is one of the most obvious characteristics of the Middle Shale Member. The assemblage is typical of the marine *Cruziana* (offshore) and *Skolithos* ichnofacies (shoreface; Seilacher, 2007) and implies oxygenated conditions at the seabed and within the water column.

The base of the sequence in Wadi Qahza represents a marked change from a thick sequence of non-bioturbated sandstones of the Lower Quartzite to the fully marine Middle Shale. The suite of pebbles and cobbles appears locally sourced and of the same provenance as that described by Lovelock *et al.* (1981) for thicker pebble beds which occur at the base of the Lower Quartzite Member. Clasts are absent through much of the Lower Quartzite re-occurring locally at the top in pebbly, cross-bedded sandstones (e.g. near base of section X). It may be that the clasts in unit 1.1 are reworked from such water-lain deposits. The minor enrichment of U in the basal coarser layers of unit 1.1 is possibly from heavy minerals (<1% in thin-section). The tabular sandstone beds in the unit are probably event beds in a shoreface environment that are later reworked by *Skolithos*, whilst the shales represent longer periods of quiet-water conditions. Where primary cross-bedding is preserved, it is current-formed, towards the NE, rather than wave-formed.

Unit 1.2 represents an increase in water depths to a more offshore setting with a reduction of sand supply. The purple colour is probably the weathering product of what were originally red sediments. These could be detrital or have formed slowly *in situ* in an oxidising environment (Ziegler & McKerrow, 1975; Turner, 1979). Shales of the subsurface Mabrouk Formation are described as red-brown in the Ghaba Salt Basin (Forbes *et al.* 2010), and marine claystones and siltstones of the Barik Sandstone Formation are red in the subsurface and at outcrop at Qarn Mahatta Humaid (Millson *et al.* 2008; Figs 1a and 2). The thin carbonate beds in unit 1.2 are developed where the interval is shaliest, with the highest

https://doi.org/10.1017/S0016756818000729 Published online by Cambridge University Press

K and Th, and where one would interpret the deepest water conditions (probably only a few tens of metres). The origin of the carbonates is unclear, given the lack of bioclasts and phosphatic residue, and the calcite mineralogy rather than ferroan calcite. They may represent bedding-parallel fracturing and fluid movement, initially of carbonate and later of quartz, either due to the release of overpressure or, perhaps more likely, during the emplacement of dolerite dikes during the Permian. Carbonate-rich fluids may have been derived from reactions with lithologies within the underlying Ediacaran Hijam Formation or the overlying Permian Saiq Formation. The carbonate-cemented layers in the Middle Shale Member have further recrystallized and become intervals of minor décollement during deep-burial and deformation in the Late Cretaceous (Figs 5b and 6b).

Unit 1.3 is a return to shallower-water shoreface conditions with most sandstones homogenized by *Skolithos* burrows. The few event beds that preserve primary stratification indicate rapid sedimentation (loading, dewatering, gutter casts) mainly from wave-influenced currents (parallel lamination and swaley cross-stratification). There were at least two minor deepening events back to purple-grey shales and *Cruziana* ichnofacies. Despite a favourable dark-grey colour of shales sampled, no acritarchs were recovered on processing, probably due to the 'overcooking' (200–300 °C) these shales were subject to in the Late Cretaceous (cf. Fraser *et al.* 2014).

Unit 2.1 is sandier and less bioturbated, but does not represent any marked shift in facies or shallow-marine environment. There is no evidence of an unconformity or a significant forced regression at its base. The thoroughly bioturbated *Daedalus* beds probably represent breaks in sedimentation of some duration.

Unit 2.2 is marked by an influx of coarser-grained, heavy mineral-rich, sand from a new or unroofed source terrain. The sandy character of much of units 2.2 and 2.4 is obscured on the GR profile by the content of heavy minerals, as in Tertiary shoreface sands of the Niger Delta that are rich in silt-sized zircons (Weber, 1971). The sandstones are shallow-water shoreface or coastal deposits with channelling, cross-stratification and thick intervals of parallel- and heavy-mineral-laminated sands, which may represent beach deposits (Clifton, 1969). The origins of the diverging palaeocurrents (100°) are not clear, but there are few other features that one might attribute to tides, or even to tide-influenced deposits (Vaucher *et al.* 2017). Sedimentation was either sufficiently rapid or conditions too hostile to prevent ubiquitous bioturbation. Quieter water periods are marked by shales with *Cruziana* or sandstones that are thoroughly bioturbated by *Daedalus* or *Skolithos*. It is not clear why *Daedalus* is more abundant in this interval than *Skolithos*, or why shelly hard parts should suddenly appear having been absent in the underlying 360 m of marine strata. It has been observed that Early Ordovician bivalves are uncommon worldwide and occur more widely in the Floian (Argentina, Morocco, Spain, France, Wales, Afghanistan? China and Australia) than they do in the Tremadocian (Argentina, France, China and Australia; Polechová, 2016).

The shaly unit 2.3 is transgressive and has the most diverse marine fauna of the Middle Shale Member. The mm-thick bivalve shell beds are interpreted as mixed assemblages transported by storm currents in an inner-shelf environment (Kidwell *et al.* 1986). With their thinness, such beds are unlikely to be resolvable by GR logs in the subsurface, though they may be apparent on micro-resistivity curves. The granule layers are also of interest with their variety of clasts that seem locally derived rather than marking erosion surfaces of more regional significance (e.g. Walker & Plint, 1992). There is no evidence that these represent fragments of hardgrounds as interpreted for some younger examples from Iran (Ghavidel-Syooki *et al.* 2014). The deepest-water conditions, though nothing deeper than *Cruziana* ichnofacies, are interpreted to be represented by the claystones and siltstones of the Ge Marker. The increase in uranium in shaly sandstones beneath this interval may be due to fluids migrating beneath a sealing lithology. The Totally Bioturbated Unit (TBU) is a dark silty sandstone that is regressive through several shallowing-upward sub-units.

Unit 2.4 is a sandy transition into the stacked, braid-delta, sandstones of Upper Quartzite Member, but still with repeated evidence of marine traces and fauna. Beds with dewatering features imply local instability caused by rapid sedimentation and high water tables. Placer concentrations of heavy minerals are parallel laminated, lensoid, occur at the tops of beds and represent marine reworking by waves in the swash zone (Clifton, 1969). The lenses may parallel the palaeo-shoreline, and their occurrence and preservation relate to washover during periods of stillstand within an overall transgression (Mattern *et al.* 2018). They do not occur at the base of channelized fluvial sandstones, along erosional discontinuities or in cross-bedded coastal-dune deposits (cf. Roy, 1999). Mattern *et al.* (2018) documented a decrease in radioactive heavy minerals in a northerly direction in the two lens-shaped placers they studied. The typically dark colour of the placers reflects an abundance of opaque minerals derived from a source terrain including igneous and metamorphic basement rocks. Other minerals are physically and chemically mature, recycled, ones in keeping with other examples from the Amdeh Formation and age equivalents in Saudi Arabia (Le Métour *et al.* 1986; Vaslet, 1990; Heward *et al.* 2018). It is thought that the increased radioactivity of Middle Shale units 2.2–2.4 is due to thorium and uranium in zircons, monazite and xenotime. A portion of the zircons are euhedral and may be derived from reworked volcanic ashes of Cambrian age.

The Shelly Marker contains bivalves that are smaller and different to the *Redonia*-like ones that occur in unit 2.3 and in younger Amdeh deposits (e.g. Am4 and Am5). The origin and implications of dolomitisation and silicification in this marker are not clear, but these aspects add to its distinctive character.

4. Evidence of the age

Trace fossils provide an indication of a Lower Ordovician age based on the types of *Cruziana* and Arthrophycid burrows present (Seilacher, 1991, 2000, 2007). There is no evidence of the distinctive Late Cambrian *Cruziana semiplicata* that is typical of the outcrops of the Al Bashair Formation at Qarn Mahatta Humaid (Fortey & Seilacher, 1997), in keeping with an observation of Fortey (1994, p. 32). Middle Shale *Cruziana* are intermediate in width (avg. 51 mm; Fig. 4), between those of the Late Cambrian Al Bashair Formation (avg. 24 mm; Fortey & Seilacher, 1997) and those in the Darriwilian Saih Nihayda Formation (avg. 88 mm; Heward *et al.*, 2018). *Cruziana omanica* is a distinctive, larger (80–90 mm), Late Cambrian form that was described by Seilacher (1962, 1970) from two specimens, collected in 1959 by Iraq Petroleum Company geologists from the Qarn Mahatta Humaid outcrops (probably from the upper part of the Al Bashair Formation; S Al-Majibi, pers. comm. 2017).

The underlying Lower Quartzite Member in Wadi Qahza contains intervals with possible microbial mat features and other 'dubio-traces', but no obviously marine ones. There is no evidence

https://doi.org/10.1017/S0016756818000729 Published online by Cambridge University Press

of the distinctive (ooidal, bioclastic and microbial) carbonates of the Late Cambrian Al Bashair Formation in the Saih Hatat outcrops, even though S Al-Marjibi (unpub. Ph.D. thesis, Univ. of Aberdeen, 2011) maps that formation extending in the subsurface along the Ghaba Salt Basin towards the NE (Fig. 1a).

Most of the fragmentary macrofossil evidence seen in the Middle Shale Member in Wadi Qahza provides little ready indication of age (bivalve moulds, inarticulate brachiopod shells, orthocone and moulds of cystoid or crinoid stem fragments, trilobite fragments, gastropod steinkerns). Pore canals, seen in trilobite sclerites in thin-section (481 m), are reported to be more common in Ordovician trilobites than they are in Cambrian ones (Horowitz & Potter, 1971). Possibly the appearance of bivalves in the sandier upper part of the Middle Shale Member marks the Floian stage as in other parts of the world (Polechová, 2016).

Le Métour *et al.* (1986) reported a fossil fauna, of interpreted Arenig–Llanvirn age (Floian–Darriwilian), from shales BRGM mapped as Am3 in Wadi Sareen (Fig. 1a; Appendix). The locality is not part of a continuous sequence and the facies differ from those in which shell beds occur in the Middle Shale Member in Wadi Qahza. The fauna of the bivalves (*Redonia*), fragmentary trilobites (*Ogyginus* and *Neseuretus*) and ribbed articulate brachiopods are the same as those mapped as Am5 just north of Wadi Sareen (Lovelock *et al.* 1981; Heward *et al.* 2018; R. Fortey, pers. comm. 2017). This leaves doubt as to whether this fossiliferous locality belongs to the Middle Shale Member (Am3) or the Upper Siltstone Member (Am5).

The Upper Siltstone Member (Am5) in Wadi Daiqa, Hayl al Quwasim and Wadi Qahza is demonstrably early to late Darriwilian in age and equivalent to the Saih Nihayda Formation in the Ghaba Salt Basin (Fig. 2; Heward *et al.* 2018). In the subsurface, it overlies the thick, sand-dominated, Ghudun Formation, which is almost certainly equivalent to the similarly thick Upper Quartzite Member (Am 4; Fig. 2). The Ghudun Formation conformably overlies the shaly Barakat and Mabrouk interval. The latter two formations have been dated as Tremadocian – possibly Floian based on acritarchs (Fig. 2; Molyneux *et al.* 2006; Forbes *et al.* 2010). It appears likely, therefore, that the Middle Shale (Am3) interval underlying the Upper Quartzite Member in the outcrops of the Amdeh Formation is the equialent of the Barakat and Mabrouk formations. If one assumes a moderately high average sedimentation rate for the sands of the Upper Quartzite of 0.1–0.2 m per 1000 years, it would have taken 8–17 Ma to have accumulated, probably corresponding to most of the 10 Ma of the Dapingian and Floian stages (Fig. 2). The subsurface Mabrouk and Barakat formations have been interpreted to contain two maximum flooding events (Droste, 1997; Molyneux *et al.* 2006; Forbes *et al.* 2010; O10 *c.* 482 Ma and O20 *c.* 478 Ma). Lovelock *et al.* (1981) also indicated two deeper-water events in the Middle Shale Member (their fig. 2), which correspond to the shaliest part of unit 1.2 and the Grey Marker of unit 2.3 of this study (Fig. 4).

The GR log profile of the type sections of the subsurface Mabrouk and Barakat formations is illustrated by well SN (Figs 8 and 1a). There is a 10–25 API positive shift between the GR of the shalier parts of the Mabrouk Formation and those of the Barakat Formation. There is a similar increase in GR of the Middle Shale outcrops between units 1.2 and 2.3 (Figs 4 and 8). The base of the Barakat Formation in the subsurface is placed at a lower GR sand, and opinions differ as to whether this is conformable or unconformable (see discussion in Forbes *et al.* 2010, pp. 204–5). The top of the Barakat Formation is considered conformable and picked at the first low-GR sandstone of the Ghudun Formation. In the outcropping Middle Shale Member, there is no evidence for an unconformity between units 1.3 and 2.1, and the whole sequence appears transitional, particularly in terms of its trace fossils and sedimentology. There is, though, a marked change in provenance with an influx of coarser, heavy-mineral-rich sand in unit 2.2. A sudden increase in thorium from spectral GR logs is also evident in the subsurface Barakat Formation (S Al-Marjibi, pers. comm. 2017). Middle Shale (Am3) units 1.1–1.3 (310 m) are interpreted as equivalent to the Mabrouk Formation, and units 2.1–2.4 (232.5 m) to the Barakat Formation (Fig. 8). The top of the Middle Shale Member is proposed to be raised from the locally occurring *Cruziana* Marker (Lovelock *et al.* 1981) to the more widespread Shelly Marker. The new position is more in keeping with the definition of the Base Ghudun Formation in the subsurface (Fig. 8; Forbes *et al.* 2010, p. 198).

The age of the underlying Lower Quartzite Member (Am2) is unclear as it contains no fossils or diagnostic trace fossils. In Wadi Qahza it has several features (GR character, grain size, multiple sets of cross-bedding up to 5+ m, lack of mud, mudclasts and mica, abundant wave ripples) that suggest it may be a coastal-dune equivalent of the Early Cambrian Amin Formation (Figs 2 and 8). If this is the case, it would imply an unconformity and a gap in the sedimentary record of >25 Ma at the base of unit 1.1 of the Middle Shale Member. The anomalous preservation of repeated intervals of wave ripples in a sandy sequence that lacks mud suggests binding by microbial mats, and there are other features and trace fossils of probable microbial origin. The Lower Quartzite Member (Am2) may represent another example of a Precambrian mat-ground survivor in the Early Cambrian (Seilacher, 2007, 2008).

If the Lower Quartzite Member (Am2) is equivalent to the subsurface Amin Formation, then it is difficult to account for the apparent absence from the outcrops of the equivalents of the Miqrat, Al Bashair and Barik formations. The Saih Hatat area probably represents the seaward continuation of the Ghaba Basin beneath the Hawasina nappes (Fig. 1a; Mount *et al.* 1998). Rising sea-levels during the Late Cambrian and Ordovician (Fig. 2) will have created accommodation space and increased the preservation potential of deposits in sedimentary basins, even in the absence of significant Ara salt in the area (Heward & Penney, 2014). The Miqrat Formation in northern Oman is interpreted to be predominantly continental and the Al Bashair, partly marine and partly continental (Forbes *et al.* 2010; S Al-Marjibi, unpub. Ph.D. thesis). The thin marine siltstones that represent the distal part of the Barik Sandstone Formation are difficult to distinguish from those of the underlying Al Bashair and the overlying Mabrouk formations (Forbes *et al.* 2010, p. 220). The seaward equivalents of these formations, if present and preserved in the Saih Hatat area, should contain fossils or trace fossils of Cambrian type. The only exploration well drilled north of the Hawasina front, AHM in Figure 1a, is thought to have drilled only as deep as the Hasirah Formation near the top of the Haima succession (Fig. 2).

5. Conodont fauna

The discovery of a fauna of platform and coniform elements is a breakthrough in allowing the direct dating of the Middle Shale Member (Am3) and confirming the palaeo-temperatures the deposits have experienced. The fauna is difficult to identify due to its limited and fragmentary nature, thermal maturity and the lack of a zonal scheme for the Gondwanan margin of the Middle East. The fauna comprises Balognathidae gen. et sp. indet. A & B, *Tetraprioniodus*, *Drepanoistodus*, *Drepanodus*, *Scolopodus*,

https://doi.org/10.1017/S0016756818000729 Published online by Cambridge University Press

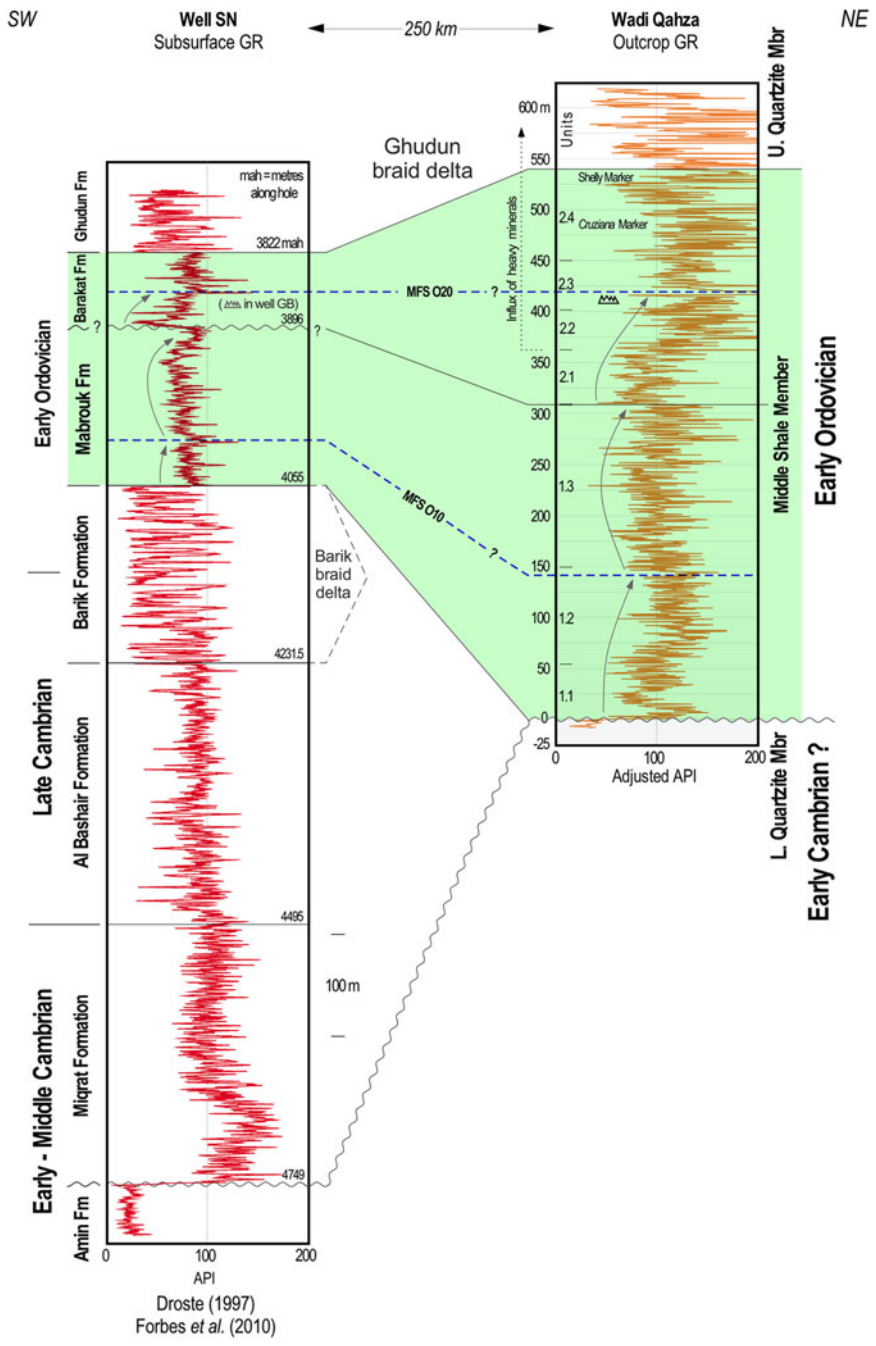

Fig. 8. Comparison of the subsurface GR log of exploration well SN and the outcrop GR recorded in Wadi Qahza. Well SN contains the type sections of the Mabrouk and Barakat formations (Forbes *et al.* 2010). The outcropping Wadi Qahza section is thicker and interpreted to be more seaward. The broad cycles around the flooding events appear to correlate, though the outcrop curve appears more serrate than that of the subsurface well.

?*Tropodus*, *Semiacontiodus*, *Teridontus* and *Erraticodon* (Fig. 7). Details of the taxonomy and age implications are discussed below.

The specimens show a conodont alteration index (CAI) of 4, higher than that calculated for Am5 deposits of Wadi Daiqa and Hayl al Quwasim (Heward *et al.* 2018), and representing palaeo-temperatures exceeding 200 °C. This would equate to 6–7 km of burial assuming a present-day surface temperature of 28 °C and a typical geothermal gradient for Oman of 30 °C/1000 m. There are no dolerite dikes near the sample location. The burial and palaeo-temperature are in keeping with zircon fission-tracks being reset at temperatures exceeding 200 °C in Am5 deposits in the headwaters of Wadis Jannah and Amdeh (Hansman *et al.* 2017) and with estimates of 275–375 °C and 6–8 kb from metamorphic minerals in the Wadi Maih sheath fold to the NE (Cornish & Searle, 2017). The maximum burial of the Amdeh sediments on the south side of Saih Hatat probably occurred during ophiolite obduction and down-flexing of the continental margin of the Arabian Plate towards a subduction zone (Searle *et al.* 2004).

5.a. Taxonomy

As the conodont fauna is limited, all platform taxa are placed in open nomenclature until more material and a better understanding of their apparatus structure is discernible. Currently two balognathid 'taxa' are identified, Balognathidae gen. et sp. indet. A and Balognathidae gen. et sp. indet. B, but the elements present may represent more than two taxa. The P elements of *Trapezognathus*, *Baltoniodus* and *Lenodus* can be difficult to distinguish (Bagnoli

https://doi.org/10.1017/S0016756818000729 Published online by Cambridge University Press

& Stouge, 1996) and the fauna contains elements that have been identified by different authors under each of these genera.

Some of the P elements identified as Balognathidae gen. et sp. indet A are similar to *Baltoniodus triangularis* (compare Fig. 7s to Carlorosi, 2013, figs 3 and 4, Carlorosi *et al.* 2013, fig. 3d). Other authors (e.g. Viira *et al.* 2001, fig. 4A–D; Carlorosi & Heredia, 2013, fig. 4a–d) have included a four-branched pastiniscaphate P element in the *Trapezognathus* apparatus, and Figure 7c and g are similar. *Trapezognathus* Lindström, 1955 has been reconstructed by Stouge & Bagnoli (1990) to include Pa, Pb, M, Sa, Sb, Sc and Sd elements, with Sd and M elements being the most characteristic (Bagnoli & Stouge, 1996). However, this apparatus reconstruction for *Trapezognathus* does not include four-branched P elements, and S Stouge & JA Rasmussen (pers. comm. 2018) suggest that Figure 7g is more likely part of the *Lenodus* apparatus. It has a better-defined cusp and is not as elongate in the centre (Fig. 7c) compared to Carlorosi *et al.* (2013, fig. 4i). Other authors, for example Carlorosi *et al.* (2013, fig. 3a, b), have chosen to include some of these elements with *Baltoniodus triangularis*. Some P elements figured under Balognathidae gen. et sp. indet. A herein (Fig. 7d, h, i) are comparable to *Fryxellodontus? corbatoi* Serpagli (1974, pl. 22, fig. 1), which was later assigned to *Polonodus? corbatoi* by Stouge & Bagnoli (1988, see pl. 10, fig. 2). Gen. et sp. indet. A by Rasmussen (2001, pl. 18, figs d, h, i) is also similar. All these elements are characterized by smoothly rounded serrations and denticles (S Stouge & JA Rasmussen, pers. comm. 2018).

P elements identified here as Balognathidae gen. et sp. indet. B (Fig. 7j, k, p, o) bear a resemblance to *Trapezognathus quadrangulum*, but are too twisted to be like Baltic examples of that taxon (S Stouge & JA Rasmussen, pers. comm. 2018). The Pb element of *Acodus deltatus* which is common in the *Paroistodus proteus* Zone, Tremadoc of Baltoscandia, is also comparable to the element figured in 7j, k, o, p (see Viira *et al.* 2006*a*, pl. 2, figs 1 and 3). We suggest it is possible that some of the distinctive quadri-ramate Sd elements with regular denticulated margins (Fig. 7l–n, q, r) are part of the Balognathidae gen. et sp. indet. B apparatus. They are similar to *Trapezognathus*, but the lack of preservation of cusps suggests a very erect element. There is slightly different denticulation on the Sd element compared with *T. quadrangulum* which shows denticulation on all four processes (Stouge & Bagnoli, 1990, p. 27), rather than three (Fig. 7m) or fewer (Fig. 7l). Fewer denticles on the upper margin of the base in the Sd element has been used to distinguish the ancestral *Trapezognathus diprion* (Lindström, 1955) from *T. quadrangulum* (Bagnoli & Stouge, 1996). Quadri-ramate S elements are present in *Aldridgeognathus manniki* (Miller *et al.* 2018) and *Baltoniodus* (see Agematsu *et al.* 2007, fig. 10.14; Tetraprioniodontiform elements of Löfgren, 1978, pl. 12; McCracken & Nowlan, 1989, pl. 1, figs 1–3, 5; Viira *et al.* 2006*b*, pl. 1, fig. 10). Van Wamel (1974, pl. 8, fig. 3 and figs ?5a, ?5b) included some similar denticulate S elements as part of the *Acodus deltatus* apparatus (as? *Baltoniodus deltatus*) but Bagnoli *et al.* (1988) do not consider them part of that apparatus. It is preferred to keep these elements in open nomenclature as they cannot clearly be shown to belong to a single apparatus or compared to isolated P elements of *Trapezognathus*, *Baltoniodus*, *Aldridgeognathus*, *Acodus* or *Lenodus*.

The platform and ramiform elements in this fauna may represent an ancestral mix of characteristics of all these genera. To test this, or to distinguish all the apparatus, M elements and more S elements are needed and further sampling is required to obtain a more extensive fauna. Rare elements have been reported and tentatively identified to generic level by other authors that could be related to those in this fauna, for example: Löfgren (1978), pl. 10, fig. 4 (Sc element), fig. 11 (Sd element), fig. 12 (Sd element, similar to *Lenodus*) and fig. 13 (Sb element) (JA Rasmussen & S Stouge, pers. comm. 2018).

The element in Figure 7u bears a resemblance to the S_3 element of *Omanognathus* (Miller *et al.* 2018, fig. 7P–R) and this is another possibility for a genus present in this fauna. However, the P elements figured here are generally more erect with better-developed cusps than *Omanognathus diaqaensis* Miller *et al.* 2018, and the element (Fig. 7u) is more likely a Pb element from the *Tetraprioniodus* apparatus (see Rasmussen, 2001, pl. 18, fig. 5 figured as *Tetraprioniodus robustus* Lindström, 1955). Clarification of this identification could be helped by finding other elements from the apparatus, particularly the M element.

Coniforms present include *Drepanoistodus*, *Drepanodus*, *Scolopodus*, ?*Tropodus* and *Semiacontiodus*. The four coniform specimens with striated bases, three of which are figured (Fig. 7w, y and aa), are the most distinctive and possibly the most useful biostratigraphically. However, they are present in small numbers, have parts of the bases and cusps missing and are too thermally mature for the white matter and extent of internal cavities to be discernible. The compressed paltodiform element (Fig. 7y) bears a resemblance to *Scolopodus striatus* as reconstructed by Tolmacheva (2006), but is considered closer to ?*Tropodus* (TY Tolmacheva, pers. comm. 2018) or *Polycostatus* (Ji & Barnes, 1996, text-fig. 13, figs 21–24). Other coniform specimens with numerous striations at the base of the cusp (Fig. 7aa) may represent a species of *Semiacontiodus* (compare Fig. 7a with Löfgren, 1999, pl. 1, fig. 2). Long-ranging coniforms include *Drepanodus* (Fig. 7x and z) and a suberectiform element of *Drepanoistodus* (Fig. 7v). An element of *Teridontus* is present (Fig. 7a, b) but the base is badly preserved and cannot be viewed in 3-D as it is embedded in sediment.

A single S_0 element was recovered (Fig. 7ac) tentatively identified as *Erraticodon* as it has distinctive, well-spaced, denticles (see Heredia *et al.* 2013, fig. 5). A similar element was described from the Am 5 Member by Miller *et al.* (2018, fig. 9f) who mentioned that this might also be classified as *Spinodus*. These types of element are rarely illustrated, difficult to place in an apparatus and currently of limited biostratigraphic use. It is hoped that similar elements will be identified and illustrated from other collections.

5.b. Interpretation of the age and 'domain'

There have been no previous attempts to provide a conodont zonal scheme for the Ordovician of the Gondwanan margin covering the Oman area as there is a lack of published and correlatable faunas (Bergström & Ferretti, 2016). The interpretation of the biostratigraphic context of this fauna therefore relies on schemes set up for other parts of the world and is hampered by the lack of taxonomic resolution and diversity in the current collection.

The platform elements identified here in open nomenclature as Balognathids (Fig. 7a–t) suggest an age no older than early Floian. The oldest balognathids known are of the genus *Zentagnathus* described from the earliest Floian *Acodus triangularis* Zone of the Acoite Formation, Cordillera Oriental, SW Argentina by Voldman *et al.* (2017). *Zentagnathus* is related to early *Baltoniodus* and *Trapezognathus*, and is like *Lenodus*, being distinguished by its tertiopedate M element (Voldman *et al.* 2017). *Trapezognathus* does not figure in the global scheme of correlation, but faunas with *Trapezognathus* have been recognized from the Lower Ordovician of Sweden (Stouge & Bagnoli, 1990); Bagnoli &

https://doi.org/10.1017/S0016756818000729 Published online by Cambridge University Press

Stouge, 1996) and Argentina (Carlorosi & Heredia, 2013). For the Argentinian region, a Floian *Trapezognathus diprion* Zone is followed by an earliest Dapingian *Baltoniodus triangularis* Zone which includes occurrences of *T. quadrangulum* (Carlorosi, 2013, fig. 5; Carlorosi & Heredia, 2013, fig. 5; Carlorosi *et al.* 2013, fig. 6). The material figured here is distinct from all known species of these genera as well as from *Zentagnathus*. The presence of an element of aff. *Erraticodon* (Fig. 7ac) also suggests a possible Floian–Dapingian age (Heredia *et al.* 2013). The remainder of the fauna suggest an earlier age. If this is the case, the balognathids illustrated here could be ancestral forms, potentially extending the first occurrence of the Family Balognathidae into the Tremadocian.

Tetraprioniodus robustus Lindström, 1955 has been recovered from the Tremadoc to earliest Floian *Paroistodus proteus* Zone of the Baltic by Löfgren (1993, 1994) and Rasmussen (2001). If Figure 7u proves comparable to Gen. et sp. indet. A. of Rasmussen (2001, pl. 18, fig. 11) this would also indicate a Tremadocian age. The tentatively identified single element of *Teridontus* (Fig. 7ab) suggests a Cambrian to Tremadocian age (see Serpagli *et al.* 2008 and references therein). The other coniforms with striated bases (Fig. 7y, w, aa) also suggest a possible Tremadocian age, although we have loosely identified them as either *Scolopodus* or *Tropodus* and *Semiacontiodus*. *Scolopodus striatus* has been found in the Lower Ordovician from the *Paroistodus proteus* Zone to the *Microzarkodina parva* Zone (Löfgren, 1978; Stouge & Bagnoli, 1990; Tolmacheva, 2006). Older examples of *Scolopodus*, for example *S.* aff. *krummi* (Lehnert, 1995), have been described from the Tremadocian–Floian Fezouata Formation of Morocco by Lehnert *et al.* (2016, fig. 3s, x). Other coniform-dominated faunas have been described from the Cambro-Ordovician of Iran (Jahangir *et al.* 2012, 2014, 2015). These faunas, particularly Tremadocian ones, contain similarly striated coniforms identified under the genera *Scolopodus* and *Tropodus* (Jahangir *et al.* 2012; TY Tolmacheva, pers. comm. 2018). Löfgren (1999, fig. 1) recognized *Semiacontiodus* from every stage of the Ordovician in the Baltic region and mentioned less differentiated examples from the late Tremadoc to Arenig in other areas of the world.

Whether this fauna proves to be Tremadocian or early Floian, it provides an interesting window on early prioniodontid conodont evolution. The chronophyletic evolutionary diagram presented by Dzik (2015, fig. 16) places *Acodus* as the basis of many Ordovician prioniodontid conodont genera with well-developed platform elements. *Trapezognathus*, *Baltoniodus* and *Lenodus* diverge from this rootstock sometime in the Floian. Stouge & Bagnoli (1999) propose a slightly earlier Tremadocian date for divergence (Miller *et al.* 2018, fig. 10).

Lehnert *et al.* (2016) described a low-diversity, coniform-dominated, fauna from the Lower Ordovician of Morocco and provided a comprehensive review of conodont faunas from the high-latitude peri-Gondwanan region (Iran, Czech Republic, France, Germany, Spain (Iberia), Belgium (eastern Avalonia), Algeria, Mexico, Colombia, Peru and NW Argentina). They defined a 'Subpolar faunal domain' which they suggest is part of the 'Cold Domain' of the 'Shallow Sea Realm' of Zhen & Percival (2003). This new domain is characterized by small numbers of widespread taxa typical of the Balto-Scandian conodont province. The Oman faunas from the Late Cambrian to the Middle Ordovician belong to this province (C Burrett, unpub. note, 1993; Bagnoli *et al.* 2016; Miller *et al.* 2018; this fauna), as does a Floian fauna from the UAE (Fortey *et al.* 2011). However, the Oman and UAE faunas also contain small numbers of platform elements such as *Baltoniodus*, *Omanognathus*, *Aldridgeogathus* and those illustrated here as Balognathids.

6. Early Ordovician (Tremadocian) rocks in Oman and the Middle East

The Mabrouk and Barakat formations that occur in the subsurface of northern Oman have been assigned to the Tremadocian based on acritarch floras (Molyneux *et al.* 2006; Forbes *et al.* 2010). Few acritarchs have been recovered from the middle and upper parts of the Barakat Formation, however, and its age has been recognized to be uncertain and possibly Floian. The only other indication of age is from a fragmentary conodont fauna of about 20 elements, obtained by crushing and heavy-liquid separation of a bioturbated dark shale parting 28 m above the base of the Barakat Formation in well GB (core 33, 3,305.86 m; HA Armstrong, unpub. report, 1993; referred to by Droste, 1997 and Forbes *et al.* 2010). There are conflicting identifications, age determinations and estimates of thermal maturity for this material by HA Armstrong (unpub. report, 1993) and C Burrett (unpub. note, 1993), and the original slide can currently not be located). Armstrong identified long-ranging coniform elements *Scalpellodus latus*, *Panderodus? sulcatus*, *Drepanoistodus* sp. indet and *Oneotodus* sp. and suggested a mid Arenig to Llanvirn age (Floian–Darriwilian). Burrett identified *Drepanodus subarcuatus* (Furnish), *Teridontus nakamurai* (Nogami) and *Teridontus quiggangensis* and suggested a mid Tremadoc age based on the range of *Teridontus*. Only the Burrett report contains photographs which appear to confirm the presence of *Teridontus*. Serpagli *et al.* (2008) have reconstructed the apparatus of *Teridontus* from the Tremadoc *Paltodus deltifer* Zone of the Montagne Noire. An acritarch flora containing *Incertae sedis* no.7 PDO and *Vulcanisphaera* spp. has been recovered from cuttings 15.5 m shallower than core 33 in well GB. Both acritarch species are considered good indicators of the Tremadocian (PDO Biozone 1108B, Forbes *et al.* 2010, pp. 172, 196).

The Barik Sandstone Formation, which underlies the Mabrouk Formation, is interpreted to range in age from the late Furongian to early Tremadocian based on trilobite evidence and context (Forbes *et al.* 2010; Fig. 2). The formation, interpreted as a braid-delta system, thins over structural highs and to the NE where it passes distally into marine siltstones (Droste, 1997; Millson *et al.* 2008; Forbes *et al.* 2010, p. 220). The Mabrouk Formation is widespread over central and north Oman and is thickest along the axis of the Ghaba Salt Basin where it can exceed 500 m (Fig. 1a; the section of well SN illustrated in Fig. 8 is relatively thin). It is described as comprising micaceous silty shales with abundant bioturbation (*Skolithos*, *Planolites*; Droste, 1997; Forbes *et al.* 2010). Molyneux *et al.* (2006) interpreted an increasingly seaward trend towards the NE based on acritarch evidence. The overlying Barakat Formation has a similar areal distribution and is about half as thick. It is again highly bioturbated (*Skolithos*, *Planolites* and *Thalassinoides*), sandier, and Lingulids and bioclasts are reported. There are no coarser-grained, more proximal, Tremadocian deposits preserved further to the south in Oman, as there are in Saudi Arabia and Jordan, though a bioturbated sandstone that occurs locally at the base of the Ghudun Formation may, in part, be equivalent (Forbes *et al.* 2010).

Deposits assigned to the Tremadocian occur widely in the Middle East, mainly in the subsurface. They are typically a few hundred metres thick, and comprise coarse-grained, pebbly, channelized, cross-bedded fluvial sandstones in the south that pass

https://doi.org/10.1017/S0016756818000729 Published online by Cambridge University Press

northwards and upwards into fine-grained marine siltstones and shales (Konert *et al.* 2001). Palaeocurrents from cross-bedded sandstones in outcrops in Jordan and Saudi Arabia are towards the north (Selley, 1972; Vaslet, 1990; Abdulkadir & Abdullatif, 2013). Marine facies are more tabular with *Skolithos* and *Cruziana* burrows (*C. furcifera*, *C. goldfussi*; Selley, 1970; Vaslet, 1990). Few fossils are reported other than acritarchs, which are often well preserved and abundant (Molyneux & Al-Hajri, 2000; Al-Hadidy, 2007; Ghavidel-Syooki & Vecoli, 2008). Only in the external terranes of Gondwana (Pontides and Taurides of Turkey and the Alborz and NE of Iran) are more diverse fossil faunas described, generally from thin bioclastic limestones that occur in shale-dominated successions (brachiopods, trilobites, conodonts and ostracods; e.g. Dean, 2004; Ghobadi Pour, 2006; Popov *et al.* 2009; Ghobadi Pour *et al.* 2011*a*, *b*; Jahangir *et al.* 2014). Reports of graptolites are rare and often from younger Floian strata (Rickards *et al.* 1994, 2010; Dean, 2004).

Ghavidel-Syooki *et al.* (2014) recovered conodonts from the Ordovician of Iran and interpreted them as late Floian based on the presence of *Baltoniodus* aff. *B. triangularis* Lindström. However, TY Tolmacheva (pers. comm. 2018), who described the conodonts, suggests that the Iranian P elements have less flared basal cavities and very small lateral extensions of the posterior process compared to the Balognathidae gen. et sp. nov. A material illustrated herein. They also suggested the horizon was equivalent to the Lower Member of the Rann Formation (Fortey *et al.* 2011). These two faunas appear to be younger than the assemblage described here which is more comparable with the *Scolopodus*/*Tropodus* fauna described by Jahangir *et al.* (2012) from the eastern Alborz, Iran (TY Tolmacheva, pers. comm. 2018).

The largely un-fossiliferous Middle Shale (Am3) outcrops of Amdeh Formation are in keeping with this regional Tremadocian–Floian context. There appears to be little difference in lithologies, trace fossils, depositional environments and water depths between the deposits of the subsurface Mabrouk and Barakat formations and those of the outcrops 250 km to the NE, implying a very low-gradient shelf system (<0.1°; as with the Darriwilian Am5, Heward *et al.* 2018). The influx of heavy minerals in the upper part of the Middle Shales appears a phenomenon limited to Oman and there is no evidence from age-equivalent deposits in Saudi Arabia that it represents a regional event (Vaslet, 1990; Knox *et al.* 2007). This switch in drainage heralds the progradation of a major braid-delta system that led to the sandstones of the Ghudun Formation / Upper Quartzite Member. The deposits of this system are three to four times the thickness of the Barik braid delta and extend much further to the south and north (Fig. 8; Droste, 1997, figs 17 and 18). The new conodont fauna is from about 100 m above the base of the likely equivalent of the Barakat Formation, approximately coeval with (or slightly younger than) the fauna interpreted by HA Armstrong (unpub. report, 1993) and C Burrett (unpub. note, 1993, fig. 8). Burrett (pers. comm. 2018) observes that the complexity of many of the elements of the new fauna suggests a Floian or younger age compared to the fauna he described in 1993.

7. Discussion

The Mabrouk Formation is an important top seal for hydrocarbon reservoirs in the underlying Barik Formation. It is likely that the 95 m shaly interval of unit 1.2 represents the sealing interval within the Mabrouk Formation (Fig. 8). The distribution of gas-condensate and oil fields within Barik Sandstone reservoirs in the Ghaba Salt Basin is limited by the northward pinch-out of sandstones within the Barik Formation (Droste, 1997, fig. 17; Millson *et al.* 2008) rather than by the extent of the Mabrouk seal. In the Fahud Salt Basin, where the Mabrouk Formation is thinner (generally <50 m; Forbes *et al.* 2010) it is likely to be a less effective seal. Sands that occur locally at the base of the Mabrouk Formation in the Ghaba Salt Basin are reported to be hydrocarbon-stained but have not yet been found to be productive commercially. They might well be for gas rather than oil. There is the potential for overlooked pay in high-GR, heavy-mineral-rich sandstones in the basal parts of the Barakat Formation, particularly in the big fields of the Ghaba area that have multiple stacked pay zones (e.g. Saih Rawl, Saih Nihayda, Barik, Mabrouk).

The accumulation and preservation of 3.4 km of Amdeh Formation in Saih Hatat is intriguing given the absence of the formation 50 km to the west in Jabal Akhdar (Fig. 1a; Mount *et al.* 1998). Droste (1997, fig. 12) provides a subsurface analogue for this with the thinning of the formations of the Haima Supergroup from the Ghaba Salt Basin onto the Makarem High. In Jabal Akhdar, any thinned deposits, as with those of later high sea-levels (Heward *et al.* 2018), must have been eroded Pre-Permian.

8. Conclusions

The Middle Shale Member (Am3) is of Early Ordovician age, probably Tremadocian–Floian, and likely to be the seaward equivalent of the Mabrouk and Barakat formations of the Ghaba Salt Basin. An abundance of marine trace fossils is characteristic of the member (*Skolithos*, *Cruziana*, *Phycodes*, *Daedalus* and *Teichichnus*). Its traces, sedimentology, conodont fauna and general lack of macrofossils are in keeping with the regional Tremadocian–Floian of the Arabian margin of Gondwana. The appearance of bivalves in the sandy upper part of the Middle Shale Member, and bioclasts in the subsurface Barakat Formation, may mark the incoming and diversification of bivalve faunas during the Floian, as in many other countries.

The base of the marine Middle Shale Member is probably unconformable on the continental/coastal Lower Quartzite Member, which may be Early–Middle Cambrian. There is no evidence of an unconformity between the shaly lower and sandy upper parts of the Middle Shale Member as has been suggested between the Mabrouk and Barakat formations in the Ghaba Salt Basin. The top of the Middle Shale Member (Am3) is proposed to be raised from the locally occurring *Cruziana* Marker to the more continuous marine interval represented by the Shelly Marker.

The most significant change in the outcrops is an influx of heavy minerals (ilmenite, anatase, zircon), which affects the GR log response of sandstones within the upper part of the member. A similar increase of GR, due primarily to thorium, occurs in the subsurface Barakat Formation. This influx possibly reflects a major change in river drainage allowing access to a source terrain which includes igneous and metamorphic basement rocks.

The recovery of conodont elements from the outcrops of the Middle Shale Member, albeit a modest one at this stage and difficult to interpret, is a breakthrough in allowing the direct dating of a further member of the Amdeh Formation. The CAI of the elements also provides further evidence of burial history and thermal conditions (>200 °C) in the SW part of Saih Hatat.

There is much potential for further study of the Middle Shale Member (Am3) its trace fossils, fauna, sedimentology, provenance, diagenesis and burial history, and for using the Amdeh outcrops as analogues for subsurface formations. Further sampling of outcrop

https://doi.org/10.1017/S0016756818000729 Published online by Cambridge University Press

and subsurface sections in Oman may provide useful information about the high-latitude origins and evolution of Ordovician platform conodonts.

There is a need to continue to improve the understanding of age and equivalence of the various parts of the Amdeh Formation, particularly the members which currently lack any direct evidence of age (Am1, 2 and 4). The Amdeh Formation should probably be elevated to group status and the existing members to formations, given its thickness and possible age range from Early Cambrian to Middle Ordovician.

Acknowledgements. This paper is dedicated to the group of enthusiastic Petroleum Development Oman (PDO) geologists who logged a 3.4 km type section through the Amdeh Formation in their weekends through 1978–9 and drew attention to its sedimentology and trace fossils.

The authors are grateful to PDO and the Ministry of Oil and Gas (Oman) for permission to include unpublished subsurface information. Mansoor Al-Jahdhami and Salah Al-Mahthori (Office for Conservation of The Environment, Diwan of Royal Court, Oman) kindly provided permission to visit locations within the Wadi Sareen Nature Reserve. We thank Willie Quizon (Petrogas E&P, Oman) for draughting, Frank Mattern and colleagues (SQU Univ., Oman) for sharing their work on Am4 heavy mineral placers, Salmeen Al-Marjibi (PDO, Oman) for data on the Al Bashair Formation from his unpublished Ph.D. thesis and comments on the subsurface, Ivan Sansom (Birmingham Univ., UK) for help with lab facilities, Malcolm Jones (PLS, Anglesey) for palynological preparations and Richard Fortey (Natural History Museum, London) for advice on the trilobites. Svend Stouge (Natural History Museum, Copenhagen), Jan Audun Rasmussen (Museum Mors, Nykøbing), Tatiana Tolmacheva (Russian Geol. Res. Inst., St Petersburg) and Gabriella Bagnoli (Univ. Pisa, Italy) provided helpful comments on the interpretation of the conodont fauna, and Clive Burrett (Mahasarakham Univ., Thailand) an improved version of the plate from his 1993 report. John Aitken and Jan Schreurs kindly reviewed drafts of the manuscript and helped improve its form and content. Clive Burrett and Bruce Levell (Oxford Univ., UK) are thanked for their careful reviews.

References

Abdulkadir IT and Abdullatif OM (2013) Facies, depositional environments, reservoir potential and palaeogeography of the Cambro-Ordovician Dibsiyah formation, Wajid outcrop belt, Saudi Arabia. *Arabian Journal of Science and Engineering* **38**, 1785–806.

Agematsu S, Sashida K, Salyapongse S and Sarsud A (2007) Ordovician conodonts from the Satun Area, Southern Peninsula Thailand. *Journal of Paleontology* **81**, 19–37.

Al-Hadidy AH (2007) Paleozoic stratigraphic lexicon and hydrocarbon habitat of Iraq. *GeoArabia* **12**, 63–130.

Aplin AC and Macquaker JHS (2011) Mudstone diversity: origin and implications for source seal and reservoir properties in petroleum systems. *Bulletin of the American Association of Petroleum Geologists* **95**, 2031–59.

Bagnoli G, Machado G and Al-Marjibi S (2016) The first record of Cambrian conodonts from the Huqf-Haushi outcrops, Oman, Arabian Peninsula. *Rivista Italiana di Paleontologia e Stratigrafia* **122**, 235–42.

Bagnoli G and Stouge S (1996) Lower Ordovician (Billingen-Kunda) conodont zonation and provinces based on sections from Horns Ude, north Öland, Sweden. *Bollettino della Società Paleontologica Italiana* **35**, 109–63.

Bagnoli G, Stouge S and Tongiorgi SM (1988) Acritarchs and conodonts from the Cambro-Ordovician Furuhäll (Köpings-klint) section (Öland, Sweden). *Rivista Italiana di Paleontologica e Stratigrafia* **94**, 163–248.

Bergström SM and Ferretti A (2016) Conodonts in Ordovician biostratigraphy. *Lethaia* **50**, 424–39.

Bottjer DJ and Droser ML (1991) Ichnofabric and basin analysis. *Palaios* **6**, 199–205.

Breton J-P, Béchennec F, Le Métour J, Moen-Maurel L and Razin P (2004) Eoalpine (Cretaceous) evolution of the Oman Tethyan continental margin: insights from a structural field study in Jabal Akhdar (Oman Mountains). *GeoArabia* **9**, 41–58.

Burkhard M (1993) Calcite twins, their geometry, appearance and significance as stress-strain markers and indicators of tectonic regime: a review. *Journal of Structural Geology* **15**, 351–68.

Carlorosi JMT (2013) La Zona de Baltoniodus triangularis (Conodonta) en el Paleozoico de la Cuenca Central Andina Sudamericana: Formación Alto del Cóndor del Norte Argentino. *Boletín Geológico y Minero* **124**, 551–62.

Carlorosi JMT and Heredia SE (2013) The Ordovician conodont Trapezognathus Lindström, 1955 in the Andean Basin, Argentina. *Neues Jahrbuch für Geologie und Paläontologie – Abhandlungen* **267**, 309–21.

Carlorosi J, Heredia S and Aceñolaza G (2013) Middle Ordovician (early Dapingian) conodonts in the central Andean Basin of NW Argentina. *Alcheringa: An Australasian Journal of Palaeontology* **37**, 299–311.

Chauvet F, Dumont T and Basile C (2009) Structures and timing of Permian rifting in the central Oman Mountains (Saih Hatat). *Tectonophysics* **475**, 563–74.

Clifton HE (1969) Beach lamination: nature and origin. *Marine Geology* **7**, 553–9.

Cornish S and Searle MP (2017) 3D geometry and kinematic evolution of the Wadi Mayh sheath fold, Oman, using detailed mapping from high-resolution photography. *Journal of Structural Geology* **101**, 26–42.

Dean WT (2004) Cambrian and Ordovician correlation and trilobite distribution in Turkey. *Fossils and Strata* **5**, 353–73.

Droste HHJ (1997) Stratigraphy of the lower Paleozoic Haima Supergroup of Oman. *GeoArabia* **2**, 419–72.

Dzik J (2015) Evolutionary roots of the conodonts with increased number of elements in the apparatus. *Earth and Environmental Science Transactions of the Royal Society of Edinburgh* **106**, 29–53.

Epstein A, Epstein JB and Harris LD (1977) Conodont color alteration – an index to thermal metamorphism. Geological Society of America Professional Paper 95, 27 pp.

Forbes GA, Jansen HSM and Schreurs J (2010) Haima Supergroup. In *Lexicon of Oman Subsurface Stratigraphy*, pp. 171–203. Manama, Bahrain: GeoArabia, Special Publication no. 5.

Fortey RA (1994) Late Cambrian trilobites from the Sultanate of Oman. *Neues Jahrbuch für Geologie und Paläontologie – Abhandlungen* **194**, 25–53.

Fortey RA, Heward AP and Miller CG (2011) Sedimentary facies and trilobite and conodont faunas of the Ordovician Rann formation, Ras al Khaimah, United Arab Emirates. *GeoArabia* **16**, 127–52.

Fortey RA and Seilacher A (1997) The trace fossil *Cruziana semiplicata* and the trilobite that made it. *Lethaia* **30**, 105–12.

Fraser WT, Watson JS, Sephton MA, Lomax BH, Harrington G, Gosling WD and Self S (2014) Changes in spore chemistry and appearance with increasing maturity. *Review of Palaeobotany and Palynology* **201**, 41–6.

Ghavidel-Syooki M, Popov LE, Álvaro JJ, Ghobadi Pour M, Tolmacheva TY and Ehsani M-H (2014) Dapingian–lower Darriwilian (Ordovician) stratigraphic gap in the Faraghan mountains, Zagros ranges, south-eastern Iran. *Bulletin of Geosciences, Czech Geological Survey* **89**, 679–706.

Ghavidel-Syooki M and Vecoli M (2008) Palynostratigraphy of middle Cambrian to lowermost Ordovician stratal sequence in the High Zagros mountains, southern Iran: regional stratigraphic implications and palaeobiogeographic significance. *Review of Palaeobotany and Palynology* **150**, 97–114.

Ghobadi Pour M (2006) Early Ordovician (Tremadocian) trilobites from Simeh-Kuh, Eastern Alborz, Iran. In *Studies in Palaeozoic Palaeontology* (eds MG Bassett and VK Deisler), pp. 93–118. Cardiff: National Museum of Wales Geological Series no. 25.

Ghobadi Pour M, Kebriaee-Zadeh MR and Popov LE (2011a) Early Ordovician (Tremadocian) brachiopods from the Eastern Alborz mountains, Iran. *Estonian Journal of Earth Sciences* **60**, 65–82.

Ghobadi Pour M, Mohibullah M, Williams M, Popov LE and Tolmacheva TY (2011b) New early ostracods from the Ordovician (Tremadocian) brachiopods of Iran: systematic, biogeographical and palaeoecological significance. *Alcheringa* **35**, 517–29.

Hansman RJ, Ring U, Thompson SN, den Brok B and Stübner K (2017) Late Eocene uplift of the Al Hajar mountains, Oman, supported by stratigraphy and low-temperature thermochronology. *Tectonics* **36**, 3081–109.

https://doi.org/10.1017/S0016756818000729 Published online by Cambridge University Press

Haq BU and Schutter SR (2008) A chronology of Paleozoic sea-level changes. *Science* **322**, 64–8.

Heredia S, Carlorosi J, Mestre A and Soria T (2013) Stratigraphical distribution of the Ordovician conodont *Erraticodon Dzik* in Argentina. *Journal of South American Earth Sciences* **45**, 224–34.

Heward AP and Penney RA (2014) Al Khlata glacial deposits in the Oman Mountains and their implications. In *Tectonic Evolution of the Oman Mountains* (eds. HR Rollinson, MP Searle, IA Abbasi, A Al-Lazki and MH Al Kindi), pp. 279–301. Geological Society of London, Special Publication no. 392.

Heward AP, Booth GA, Fortey RA, Miller CG and Sansom IJ (2018) Darriwilian shallow-marine deposits from the Sultanate of Oman, a poorly known portion of the Arabian margin of Gondwana. *Geological Magazine* **155**, 59–84.

Horowitz AS and Potter PE (1971) *Introductory Petrography of Fossils*. New York: Springer-Verlag, 302 pp.

Hughes Clarke MW (1988) Stratigraphy and rock unit nomenclature in the oil-producing area of interior Oman. *Journal of Petroleum Geology* **11**, 5–60.

Jahangir H, Ghobadi Pour M, Ashuri A-R and Amini A (2015) Terminal Cambrian and early Ordovician (Tremadocian) conodonts from Eastern Alborz, north-central Iran. *Alcheringa* **40**, 219–43.

Jahangir H, Ghobadi Pour M, Holmer LE, Popov LE, Ashuri A-R, Rushton A, Tolmacheva TY and Amini A (2014) Biostratigraphy of the Cambrian-Ordovician boundary beds at Kopet-Dagh, Iran. *Stratigraphy* **12**, 40–7.

Jahangir H, Ghobadi Pour M, Tolmacheva TY, Popov L and Hosseini-Nezhad M (2012) Conodont and trilobite biostratigraphy across the Cambrian-Ordovician boundary in Deh-Molla eastern Alborz, Iran. *Palaeontological Association Newsletter* **81**, 70–1.

Ji Z and Barnes CR (1996) Uppermost Cambrian and lower Ordovician conodont biostratigraphy of the survey peak formation (Ibexian/Tremadoc), Wilcox Pass, Alberta, Canada. *Journal of Paleontology* **70**, 871–90.

Kidwell SM, Fursich FT and Aigner T (1986) Conceptual framework for the analysis and classification of fossil concentrations. *Palaios* **1**, 228–38.

Knox RWO'B, Franks SG and Cocker JD (2007) Stratigraphic evolution of heavy-mineral provenance signatures in the sandstones of the Wajid group (Cambrian to Permian), southwestern Saudi Arabia. *GeoArabia* **12**, 65–96.

Konert G, Afifi AA, Al-Hajri SA and Droste HJ (2001) Paleozoic stratigraphy and hydrocarbon habitat of the Arabian plate. *GeoArabia* **6**, 407–42.

Lehnert O (1995) Ordovizische Conodonten aus der Präkordillere Westargentiniens: Ihre Bedeutung für Stratigraphie und Paläogeographie. *Erlanger Geologische Abhandlung* **125**, 1–193.

Lehnert O, Nowak H, Sarmiento GN, Gutiérrez-Marco JC, Akodad M and Servais T (2016) Conodonts from the lower Ordovician of Morocco – contributions to age and faunal diversity of the Fezouata Lagerstätte and peri-Gondwana biogeography. *Palaeogeography, Palaeoclimatology, Palaeoecology* **460**, 50–61.

Le Métour J, Villey M and De Gramont X (1986) *Geological Map of Qurayat, Sheet NF 40-4D, Scale 1:100,000. Explanatory Notes*. Oman: Directorate General of Minerals, Oman Ministry of Petroleum and Minerals, 72 pp.

Lindström M (1955) Conodonts from the lowermost Ordovician strata of south-central Sweden. *Geologiska Föreningens i Stockholm Förhandlingar* **76**, 517–604.

Löfgren A (1978) Arenigian and Llanvirnian conodonts from Jämtland, northern Sweden. *Fossils and Strata* **13**, 129.

Löfgren A (1993) Conodonts from the lower Ordovician at Hunneberg, south-central Sweden. *Geological Magazine* **130**, 215–32.

Löfgren A (1994) Arenig (lower Ordovician) conodonts and biozonation in the eastern Siljan district, central Sweden. *Journal of Paleontology* **68**, 1350–68.

Löfgren A (1999) The Ordovician conodont *Semiacontiodus cornuformis* (Sergeeva, 1963). *Geologica et Palaeontologica* **33**, 71–91.

Lovelock PER, Potter TL, Walsworth-Bell EB and Wiemer WM (1981) Ordovician rocks in the Oman mountains: the Amdeh formation. *Geologie en Mijnbouw* **60**, 487–95. (Also 1:1000 Composite Section, Amdeh Formation, Wadi Kahza – Wadi Amdeh, Saih Hatat, 1979, unpublished).

Mattern F, Pracejus B and Al-Balushi L (2018). Heavy mineral beach placers of the Ordovician Amdeh formation (Member 4, Wadi Qahza, Saih Hatat, eastern Oman Mountains): where is the main source area? *Journal of African Earth Sciences* **147**, 633–46.

McCracken A and Nowlan G (1989) Conodont paleontology and biostratigraphy of Ordovician and petroliferous carbonates from Southampton, Baffin and Aptapok islands in the eastern Canadian Arctic. *Canadian Journal of Earth Sciences* **26**, 1880–903.

Miller CG, Heward AP, Mossoni A and Sansom IJ (2018). Two new early balognathid conodont genera from the Ordovician of Oman and comments on the early evolution of prioniodontid conodonts. *Journal of Systematic Palaeontology* **16**, 571–93.

Millson JA, Quin JG, Idiz E, Turner P and Al-Harthy A (2008) The Khazzan gas accumulation, a giant combination trap in the Cambrian Barik Sandstone member, Sultanate of Oman: implications for Cambrian petroleum systems and reservoirs. *Bulletin of the American Association of Petroleum Geologists* **92**, 885–917.

Molyneux SG and Al-Hajri S (2000) Palynology of a problematic Lower Palaeozoic lithofacies in central Saudi Arabia. In *Stratigraphic Palynology of the Palaeozoic of Saudi Arabia* (eds S Al-Hajri and B Owens), pp. 18–41. Manama, Bahrain: GeoArabia Special Publication no. 1.

Molyneux SG, Osterloff P, Penney RA and Spaak P (2006) Biostratigraphy of the lower Palaeozoic Haima supergroup, Oman; its application in sequence stratigraphy and hydrocarbon exploration. *GeoArabia* **11**, 17–48.

Mount VS, Crawford RIS and Bergman SC (1998) Regional structural style of the central and southern Oman mountains: Jebel Akhdar, Saih Hatat and the northern Ghaba Salt basin. *GeoArabia* **3**, 475–90.

Morton DM (1959) The geology of Oman. *Proceedings of the 5th World Petroleum Congress*, vol. **1**, pp. 277–94. New York.

Polechová M (2016) The bivalve fauna from the Fezouata formation (lower Ordovician) of Morocco and its significance for palaeobiogeography, palaeoecology and early diversification of bivalves. *Palaeogeography, Palaeoclimatology, Palaeoecology* **460**, 155–69.

Popov LE, Ghobadi Pour M, Bassett MG and Kebriaee-Zadeh MR (2009) Billingsellide and orthide brachiopods: new insights into earliest Ordovician evolution and biogeography from Northern Iran. *Palaeontology* **52**, 35–52.

Rasmussen JA (2001) Conodont biostratigraphy and taxonomy of the Ordovician shield margin in the Scandinavian Caledonides. *Fossils and Strata* **48**, 1–180.

Rickards BR, Booth GA, Paris F and Heward AP (2010) Marine flooding events of the early and middle Ordovician of Oman and the United Arab Emirates and their graptolite, acritarch and chitinozoan associations. *GeoArabia* **15**, 81–120.

Rickards BR, Hamedi MA and Wright AJ (1994) A new Arenig graptolite fauna from the Kerman district, east-central Iran. *Geological Magazine* **131**, 35–42.

Roy PS (1999) Heavy mineral beach placers in southeastern Australia; their nature and genesis. *Economic Geology* **94**, 567–88.

Saddiqi O, Michard A, Goffe B, Poupeau G and Oberhänsli R (2006) Fission-track thermochronology of the Oman mountains continental windows, and current problems of tectonic interpretation. *Bulletin de la Société géologique de France* **177**, 127–34.

Searle MP, Warren CJ, Waters DJ and Parish RR (2004) Structural evolution of the Arabian continental margin, Saih Hatat region, Oman mountains. *Journal of Structural Geology* **26**, 451–73.

Seilacher A (1962) Form und Function des Trilobiten-daktylus. *Paläontologische Zeitschrift* **36**, 218–27.

Seilacher A (1970) Cruziana stratigraphy of 'non-fossiliferous' Palaeozoic sandstones. In *Trace Fossils* (eds TP Crimes and JC Harper), pp. 447–76. Geological Journal Special Issue no. 3. Liverpool: Seel House Press.

Seilacher A (1991) An updated Cruziana stratigraphy of Gondwanan Palaeozoic sandstones. In *The Geology of Libya IV* (eds MJ Salem, OS Hammuda and BA Eliagoubi), pp. 1565–81. Amsterdam: Elsevier.

Seilacher A (2000) Ordovician and Silurian arthrophycid ichnostratigraphy. In *Geological Exploration in Murzuq Basin* (eds MA Sola and D Worsley), pp. 237–58. Amsterdam: Elsevier Science B.V.

Seilacher A (2007) *Trace Fossil Analysis*. Berlin; Heidelberg: Springer-Verlag, 226 pp.

Seilacher A (2008) *Fossil Art*. Laasby: CBM-Publishing, 102 pp.

Selley RC (1970) Ichnology of Palaeozoic sandstones in the southern Desert of Jordan: a study of trace fossils in their sedimentological context. In *Trace*

Fossils (eds TP Crimes and JC Harper), pp. 477–88. Geological Journal Special Issue no. 3. Liverpool: Seel House Press.

Selley RC (1972) Diagnosis of marine and non-marine environments from the Cambro-Ordovician sandstones of Jordan. *Journal of the Geological Society* **128**, 135–50.

Serpagli E (1974) Lower Ordovician conodonts from precordilleran Argentina (province of San Juan). *Bollettino della Società Paleontologica Italiana* **13**, 17–98.

Serpagli E, Ferretti A, Nicoll RS and Serventi P (2008) The conodont genus *Teridontus* (Miller, 1980) from the early Ordovician of the Montagne Noire, France. *Journal of Paleontology* **82**, 612–20.

Stouge S and Bagnoli G (1988) Early Ordovician conodonts from the Cow Head Peninsula, western Newfoundland. *Palaeontographia Italica* **75**, 89–179.

Stouge S and Bagnoli G (1990) Lower Ordovician (Volkhovian-Kundan) conodonts from Hagudden, northern Öland, Sweden. *Palaeontographia Italica* **77**, 1–54.

Stouge S and Bagnoli G (1999) The suprageneric classification of some Ordovician prioniodontid conodonts. *Bollettino della Società Paleontologica Italiana* **37**, 145–58.

Tolmacheva TY (2006) Apparatus of the conodont *Scolopodus striatus* Pander, 1856 and a re–evaluation of Pander's species of *Scolopodus*. *Acta Palaeontologica Polonica* **51**, 247–60.

Turner P (1979) Diagenetic origin of Cambrian marine red beds: Caerfai Bay Shales, Dyfed, Wales. *Sedimentary Geology* **24**, 269–81.

van Wamel WA (1974) Conodont biostratigraphy of the upper Cambrian and lower Ordovician of north western Öland. *Utrecht Micropalaeontological Bulletins* **10**, 126.

Vaslet D (1990) Le Paléozoïque (anté-Permien supérieur) d'Arabie Saoudite. Document du BRGM no. 191, 209 pp.

Vaucher R, Pittet B, Hormière H, Martin LO and Lefebvre B (2017) A wave-dominated, tide-modulated model for the lower Ordovician of the Anti-Atlas, Morocco. *Sedimentology* **64**, 777–807.

Viira V, Aldridge RJ and Curtis S (2006a) Conodonts of the Kiviõli member, Viivikonna formation (upper Ordovician) in the Kohtla section, Estonia. *Proceedings of the Estonian Academy of Science, Geology* **55**, 213–40.

Viira V, Mens K and Nemliher J (2006b) Lower Ordovician Leetse formation in the North Estonian Klint area. *Proceedings of the Estonian Academy of Science, Geology* **55**, 156–74.

Viira V, Löfgren A, Mägi S and Wickström J (2001) An early to middle Ordovician succession of conodont faunas at Mäekalda, northern Estonia. *Geological Magazine* **138**, 699–718.

Villey M, Le Métour J and De Gramont X (1986) *Geological Map of Fanjah, Sheet NF 40-3F, Scale 1:100,000. Explanatory Notes*. Oman: Directorate General of Minerals, Oman Ministry of Petroleum and Minerals, 68 pp.

Voldman GG, Albanesi GL, Ortega G, Giuliano ME and Monaldi CR (2017) New conodont taxa and biozones from the lower Ordovician of the Cordillera Oriental, NW Argentina. *Geological Journal* **52**, 394–414.

Walker RG and Plint AG (1992) Wave and storm-dominated shallow marine systems. In *Facies Models: Response to Sea Level Change* (eds RG Walker and NP James), pp. 219–38. Toronto: Geological Association of Canada.

Weber KJ (1971) Sedimentological aspects of the oil fields in the Niger delta. *Geologie en Mijnbouw* **50**, 559–76.

Wellman CH, Osterloff PL and Mohiuddin U (2003) Fragments of the earliest land plants. *Nature* **425**, 282–5.

Zhen YY and Percival IG (2003) Ordovician conodont biogeography – reconsidered. *Lethaia* **36**, 357–70.

Ziegler AM and McKerrow WS (1975) Silurian marine red beds. *American Journal of Science* **275**, 31–56.

Appendix

Coordinates of the sections and locations sampled for conodonts and palynology in Wadi Qahza. BRGM fossil location in Wadi Sareen discussed in text, possibly Am5 (Upper Siltstone Member) rather than Am3 (Middle Shale Member).

	Lat.	Long.		Lat.	Long.	Comments
Wadi Qahza						
Base X	23°18′54.2″	58°22′52.0″	Base A	23°19′23.6″	58°22′16.4″	
Top X	23°18′59.5″	58°22′49.3″	Top A	23°19′25.6″	58°22′10.2″	
Base Y	23°19′15.6″	58°22′52.2″	Base B	23°18′15.7″	58°22′23.2″	
Top Y	23°19′37.6″	58°22′14.2″	Top B	23°18′19.0″	58°22′17.5″	
Base A0	23°19′27.9″	58°22′17.7″	Base C	23°18′6.9″	58°22′11.3″	
Top A0	23°19′27.8″	58°22′15.0″	Top C	23°18′4.9″	58°22′25.7″	
Conodont samples						
Sect Y, Carb 4, Y7	23°19′26.8″	58°22′41.9″	Sect A, 16/1	23°19′24.5″	58°22′11.8″	Bivalves
Sect Y, Carb 5, Y2	23°19′26.4″	58°22′41.7″	Sect B, 16/5	23°18′17.4″	58°22′20.1″	Bivalves, brachiopods, conodonts
			Sect C, 16/6	23°18′11.8″	58°22′20.1″	Bivalves
Palynology samples			**Wadi Sareen**			
Sect Y, Y9P	23°19′35.9″	58°22′28.0″	BRGM Fossil Location	23°13′18.0″	58°36′17.9″	Bivalves, trilobites, brachiopods
Sect Y, Y10P	23°19″39.3″	58°22′21.3″				
Sect Y, Y11P	23°19′36.1″	58°22′20.9″				

https://doi.org/10.1017/S0016756818000729 Published online by Cambridge University Press